1 **Regulation of late-acting operons by three transcription factors and a CRISPR-Cas component**

2 **during *Myxococcus xanthus* development**

3 **Shreya Saha and Lee Kroos***

4 *Department of Biochemistry and Molecular Biology*, *Michigan State University*, *East Lansing*, *MI*

5 *48824*, *USA.*

6 Running title: Complex regulation of sporulation genes during *M. xanthus* development

7 *For correspondence. E-mail kroos@msu.edu; Tel. (+1) 517 355 9726; Fax (+1) 517 353 9334.

8

Abstract

Starvation induces *Myxococcus xanthus* multicellular development. Rod-shaped cells move, forming mounds. Within mounds, rods differentiate into round, stress-resistant spores. C-signaling is proposed to activate FruA, which binds DNA cooperatively with MrpC to increase transcription of many genes. We report that the regulation of late-acting operons involved in spore metabolism (*fadIJ*) and coat biogenesis (*exoA-I*, *exoL-P*, *nfsA-H*) is more complex. These operons appear to be negatively regulated by FruA prior to its activation, then positively regulated by C-signal-activated FruA, based on transcript levels in mutants. Although MrpC is required to produce FruA, loss of MrpC affected transcript levels differentially. Transcript measurements also indicated that transcription factor Nla6 is a positive regulator of late-acting operons, whereas the DevI component of a CRISPR-Cas system is a negative regulator. FruA bound to all four promoter regions *in vitro*, but each promoter was unique in terms of whether or not MrpC and/or Nla6 bound, and in terms of cooperative binding. Whereas FruA switches from negative to positive regulation of all four operons temporally, MrpC and Nla6 appear to exert operon-specific temporal regulation. We propose that complex, differential regulation of late-acting operons ensures that spore resistance and surface characteristics meet environmental demands.

Author Summary

Starving *Myxococcus xanthus* bacteria coordinate their movements to build multicellular mounds on a solid surface. Within the mounds rod-shaped cells transform into round spores that can survive starvation and other harsh conditions. Thousands of genes must be properly regulated in response to many signals to complete this developmental process. We investigated the regulation of genes whose products act near the end of the process to change metabolism of the spore and protect its contents by depositing a polysaccharide coat on its surface. We discovered that the regulation of these genes is unusually complex. It involves three transcription factors that respond to different signals and bind to the promoter regions in different combinations. This allows each promoter to be regulated uniquely. Combinatorial regulation of this complexity is common in higher eukaryotes, but not in bacteria. In addition, all the promoters are controlled by a CRISPR-Cas system. These systems typically defend bacteria against viral infection. Our results suggest that *M. xanthus* evolved complex eukaryotic-like combinatorial control of transcription and a link to a CRISPR-Cas system to thwart viral intrusion while making spores suited suited to withstand starvation and environmental insults.

44 **Introduction**

45 The Gram-negative soil bacterium *Myxococcus xanthus* provides an attractive model system to
46 study signal-induced gene regulation and bacterial community behavior (1). Upon nutrient
47 depletion, cells move on solid surfaces and form mounds, within which some of the rod-shaped
48 cells differentiate into round, stress-resistant spores. During this multicellular developmental
49 process of fruiting body formation, a majority of the population undergoes lysis, while some
50 cells remain outside of fruiting bodies as peripheral rods (2, 3).

51 A signal-responsive gene regulatory network governs the developmental process of *M.*
52 *xanthus* (4). Starvation triggers production of the intracellular secondary messenger molecules
53 (p)ppGpp (5, 6) and c-di-GMP (7), which lead to production of the extracellular A- and C-signals
54 (5, 8-10) and exopolysaccharide (7), respectively. The short-range C-signal appears to be a
55 proteolytic fragment of the CsgA protein (11-13) and/or diacylglycerols produced by cardiolipin
56 phospholipase activity of full-length CsgA (14), but the mechanisms of signal transduction
57 remain to be elucidated. C-signaling appears to posttranslationally activate the transcription
58 factor FruA (15, 16), but the mechanism is unknown. FruA is similar to response regulators of
59 two-component signal-transduction systems (17). Response regulators are typically activated
60 by phosphorylation by a histidine kinase (15). However, for several reasons, phosphorylation is
61 unlikely to be the mechanism by which FruA is activated in response to C-signaling (16, 18).

62 Transcription of the *fruA* gene is regulated by a cascade of starvation-responsive
63 transcription factors that includes MrpC (4, 19), which binds upstream of the *fruA* promoter and
64 stimulates transcription (20, 21). In addition to transcriptional control of the *mrpC* gene by
65 starvation (22), the level of MrpC protein is regulated by proteolysis, slowing the pace of

66 development under the normal conditions of starvation (23, 24) and halting development if
67 sufficient nutrients are added back before rods become committed to spore formation (25, 26).
68 *In vitro*, MrpC and FruA bind cooperatively to the promoter regions of many
69 developmentally-regulated genes (27). Mutational analyses of five such promoter regions
70 suggest that cooperative binding to a site just upstream of the promoter stimulates
71 transcription *in vivo*, whereas binding to nearby sites can increase or decrease transcription (18,
72 28-31). The different arrangements of binding sites with different affinities for MrpC and FruA
73 may explain the observed differences between genes in terms of their spatiotemporal patterns
74 of expression and their extent of dependence on C-signaling for expression (4, 32, 33). The
75 levels of MrpC, FruA, and CsgA normally rise in starving rods engaged in mound building (3), but
76 the addition of sufficient nutrients triggers rapid proteolysis of MrpC and prevents the normal
77 increase in transcripts for proteins involved in sporulation (25, 26). Combinatorial control of
78 gene expression by MrpC and FruA appears to ensure that only starving rods (in which MrpC
79 and FruA are synthesized and stably accumulate) aligned in mounds (which enhances short-
80 range C-signaling between rods, presumably activating FruA within them) commit to spore
81 formation (4, 18, 25, 33, 34).
82 Among the genes combinatorially controlled by MrpC and FruA (28), early studies showed
83 that mutations in the *dev* operon can cause severe defects in sporulation (35-38). The *dev*
84 operon includes eight genes comprising a CRISPR-Cas system that may protect developing *M.*
85 *xanthus* against phage infection (39). The first gene in the *dev* operon, *devI*, codes for a 40-
86 residue protein that strongly inhibits sporulation when overproduced (40), delays sporulation
87 by about 6 h when produced at the normal level (16, 41), and exerts weak positive

88 autoregulation on *dev* transcript accumulation (16). In contrast, in-frame deletions in three
89 genes of the *dev* operon (*devTRS*) increase accumulation of the *dev* transcript 10-fold during
90 development (16, 40, 41), indicating that DevTRS proteins exert strong negative autoregulation.
91 The negative autoregulation by DevTRS proteins is crucial in order to prevent DevI
92 overproduction from inhibiting sporulation (40, 41).

93 The products of several other operons act late during the developmental process, impacting
94 the metabolism of nascent spores and the biogenesis of their coat polysaccharide, but the
95 regulation of these operons is not fully understood. The putative *fadIJ* operon is normally
96 induced twofold in sporulating cells, but not in *csgA*, *fruA*, or *mrpC* mutants (42). Recently
97 published data support that *fadIJ* are co-transcribed as an operon (43). FadIJ are enzymes in a
98 fatty acid β-oxidation pathway that impacts spore structure and resistance properties (42). The
99 *nfsA-H* operon is up-regulated in spores formed during the starvation-induced developmental
100 process and in spores induced artificially by glycerol addition (44). The starvation-induced up-
101 regulation fails in a *csgA* mutant, is diminished in a *devRS* mutant, and, unusually, is greater in a
102 *fruA* mutant, suggesting negative regulation by FruA (44). The NfsA-H proteins form a complex
103 involved in biogenesis of the coat polysaccharide to generate compact and rigid stress-resistant
104 spores (45-47). The *exoA-I* operon (45) is normally induced late in development, but not in *csgA*
105 or *devRS* mutants (48). Transcription depends on binding of FruA (49) and Nla6 (50) to the
106 *exoA-I* promoter region. Interestingly, Nla6 is part of a cascade of enhancer-binding proteins
107 that responds to starvation early in development (19) and leads to production of MrpC and
108 FruA (4). Nla6 also binds to the promoter region of the predicted *MXAN_3259–MXAN_3263*
109 operon and appears to directly regulate transcription (50). Recently published data support

110 that the five genes are co-transcribed as an operon (43), which was renamed the *exoL-P* operon
111 based on functional studies (51). The ExoA-I and ExoL-P proteins are involved in the synthesis,
112 export, and modification of the spore coat polysaccharide (45, 46, 51).
113 Here, we report systematic investigation of the late-acting *fadIJ*, *nfsA-H*, *exoA-I*, and *exoL-P*
114 operons with respect to the phenotypes of mutants and the regulation of gene expression. We
115 found that *exo* mutants exhibit stronger defects in sporulation than an *nfs* mutant, whereas an
116 *fad* mutant exhibited very little difference from a "wild-type" (WT) strain under our conditions.
117 Cooperative binding of MrpC and FruA appears to stimulate transcription of *fadIJ*, but
118 regulation of *fadIJ* as well as *nfsA-H*, *exoA-I*, and *exoL-P* involves additional complexities, with
119 FruA acting negatively prior to its activation and then C-signal-activated FruA acting positively
120 later in development. Binding of MrpC appears to stimulate transcription of *nfsA-H* and *exoL-P*,
121 albeit with some notable differences, and MrpC appears to indirectly decrease the *exoA*
122 transcript level. Nla6 is a positive regulator of the late-acting operons early in development and
123 binds cooperatively with FruA to the *nfsA-H*, *exoL-P*, and *exoA-I* promoter regions, and also
124 binds cooperatively with MrpC to the *nfsA-H* promoter region. The DevI CRISPR-Cas component
125 is a negative regulator of the late-acting operons. We conclude that three transcription factors
126 and a CRISPR-Cas component regulate the late-acting operons and we propose that complex,
127 differential regulation of genes involved in spore metabolism and coat biogenesis produces
128 spores suited to withstand environmental insults.
129

130 **Results**

131 **Mutations in *exo* genes impair sporulation more strongly than deletion of the *nfs* operon**

132 In previous work, we established methods to systematically analyze *M. xanthus* development
133 under submerged culture conditions (16). Submerged culture involves growing cells in nutrient
134 medium followed by sedimentation, resuspension in starvation buffer, and incubation in a
135 plastic container. Cells attach to the container bottom and develop under a layer of buffer.
136 Here, we examined the developmental time course of *exo*, *nfs*, and *fad* mutants microscopically
137 and by harvesting samples for cellular and molecular analyses.

138 We compared submerged culture development of mutants with that of WT laboratory
139 strain DK1622 (52) from which the mutant strains were derived. Specifically, we examined the
140 effects of an insertion in *fadI* (42), a deletion of the entire *nfsA-H* operon (44), an insertion in
141 *exoC* (45, 48), and an insertion in *exoL* (50, 51). As expected (16), the WT strain formed mounds
142 by 18 h poststarvation (PS) and the mounds began to darken by 30 h (Fig. 1). Darkening
143 typically correlates with spore formation. The *fadI* mutant was indistinguishable from the WT
144 strain. The *nfsA-H* mutant was delayed by about 3 h in mound formation and appeared to be
145 delayed and reduced in mound darkening. The *exoC* and *exoL* mutants formed normal-looking
146 mounds by 18 h, but subsequent mound darkening was reduced compared to the WT strain,
147 suggesting sporulation defects.

148 To quantify changes at the cellular level, we harvested samples from submerged culture and
149 either treated the samples with glutaraldehyde to fix cells or left the samples untreated (16).
150 Using the untreated samples, we quantified "sonication-resistant spores" microscopically and
151 "mature spores" that were heat- and sonication-resistant and capable of germination and
152 colony formation on nutrient agar. We used the fixed samples to quantify "sonication-sensitive
153 cells" microscopically (i.e., the total number of cells observed in the fixed sample minus the

154 number of sonication-resistant spores observed in the corresponding untreated sample). The
155 vast majority of sonication-sensitive cells were rod-shaped, but we also observed a small
156 percentage of "transitioning cells" (TCs) intermediate in morphology between rods and spores
157 (33) in some of the fixed samples.

158 As expected (16), we first observed sonication-resistant spores at 27 h PS in samples of the
159 WT strain, and the spores rose from ~0.2% (as a percentage of the number of rod-shaped cells
160 present at T_0, the time starvation initiated development) to ~2% at 48 h (Fig. 2). The *fadI*
161 mutant formed more spores than the WT strain. Consistent with the observed mound
162 darkening defects (Fig. 1), the *nfsA-H* mutant formed less spores than the WT strain, and the
163 *exoC* and *exoL* mutants did not form spores (at a detection limit of 0.05% of the T_0 cell number)
164 (Fig. 2 and Table S1). Neither did the *exoC* and *exoL* mutants form mature spores at 72 h (at a
165 detection limit of 0.00001% of the T_0 cell number), while the *nfsA-H* mutant made ~15% as
166 many mature spores as the WT strain, and the *fadI* mutant made a similar number of mature
167 spores as the WT strain (Table S1).

168 The WT strain exhibited a decline of sonication-sensitive cells during development similar to
169 that reported previously (16), with only ~30% of the T_0 cell number remaining at 18 h PS and
170 only ~6% remaining at 48 h (Fig. S1A). It was also reported previously that the decrease in cell
171 number correlates with a decrease in the total protein concentration of developing cultures,
172 which was suggested to reflect lysis of the majority of cells early during development under
173 submerged culture conditions (25). The mutants showed similar decreases in cell number as
174 the WT strain (Fig. S1A). As noted above, we observed a small percentage of TCs in some of the
175 fixed samples. For the WT strain, ~3% of the T_0 cell number were TCs at 24 h (Fig. S1B), when

176 sonication-sensitive cells were ~20% of the T_0 cell number (Fig. S1A). Thus, TCs comprised 15%
177 of the total population at 24 h, before sonication-resistant spores were observed (Fig. 2), in
178 agreement with *in situ* observations using confocal microscopy (33). The percentage of TCs
179 decreased at later times (Fig. S1B), presumably as TCs became sonication-resistant spores (Fig.
180 2). The *fadI* mutant showed about half as many TCs as the WT strain at most time points (Fig.
181 S1B), perhaps due to the *fadI* mutant forming more sonication-resistant spores (Fig. 2). The *exo*
182 and *nfs* mutants exhibited less TCs at 24 h (~0.4-0.7% of the T_0 cell number), but in each case
183 the percentage rose to at least 1% later (Fig. S1B), suggesting that these mutants begin to
184 change shape, but are impaired in their ability to make spores.
185 We conclude that the *exoC* and *exoL* mutants exhibited stronger defects in sporulation than
186 the *nfsA-H* mutant, whereas the *fadI* mutant exhibited very little difference from the WT strain
187 under our conditions.
188
189 **Transcript levels from the late-acting operons are very low in the absence of C-signaling**
190 We used methods established previously (16) to measure transcript levels from the late-acting
191 operons of the WT strain and a *csgA* insertion mutant at 18-30 h PS, the period leading up to
192 and including the time that many cells commit to spore formation and sonication-resistant
193 spores begin to be observed (25) (Fig. 2). As expected for the WT strain (26), transcript levels
194 rose during development (Fig. 3). As noted previously (41), the *exoA* transcript level varied
195 greatly between biological replicates (Fig. 3A), which we do not understand. The *exoL*
196 transcript level likewise varied greatly (Fig. 3B). The *nfsA* (Fig. 3C) and *fadI* (Fig. 3D) transcript

197 levels varied less and on average increased only ~fourfold, much less than the *exoA* (~24-fold)
198 and *exoL* (~70-fold) transcript levels.

199 For the *csgA* mutant, which is unable to produce C-signal, the transcript levels did not
200 increase during development (Fig. 3, asterisks indicate $p < 0.05$ in Student's two-tailed *t*-tests
201 comparing the mutant to the WT strain at each time point). Asterisks are absent above the
202 *exoA* and *exoL* transcript levels of the *csgA* mutant because the statistical test yielded $p > 0.05$
203 due to the large variation between biological replicates of the WT strain. Nevertheless, the
204 *exoA* and *exoL* transcript levels of the *csgA* mutant were low for all replicates at each time
205 point. We conclude that transcript levels from the late-acting operons are very low in the
206 absence of C-signaling. In agreement, reporter activity from fusions to *exoC* (48), *nfsA* (44), and
207 *fadI* (42) was very low for *csgA* mutants relative to WT strains during development.

208 The low transcript levels could be due to decreased synthesis and/or increased degradation
209 in the *csgA* mutant compared with the WT strain. To measure the transcript degradation rates,
210 we added rifampicin to inhibit transcription at 30 h PS and determined the transcript levels at
211 intervals thereafter. The transcript degradation rates did not differ significantly between the
212 *csgA* mutant and the WT strain (Fig. 4), suggesting that decreased synthesis primarily accounts
213 for the low transcript levels in the absence of C-signaling.

214 Considerable evidence supports a model in which C-signaling activates FruA
215 posttranslationally in order to increase transcription of genes during *M. xanthus* development
216 (15, 16). We showed previously that the FruA level of a *csgA* mutant is about twofold lower
217 than that of the WT strain at 18-30 h PS (16). Boosting the FruA level in the *csgA* mutant to the
218 WT level using a vanillate-inducible promoter (P_{van}) fused to *fruA* did not increase the transcript

219 levels of five genes or operons (*dev*, *fmgA*, *fmgBC*, *fmgD*, and *fmgE*) known to be under
220 combinatorial control of FruA and MrpC. Neither did boosting the level of FruA D59E (with a
221 phosphomimetic substitution in its receiver domain) using a P_{van}-*fruA D59E* fusion.
222 We tested whether boosting the level of FruA or its D59E variant in the *csgA* mutant
223 increases the transcript levels of the late-acting operons. The transcript levels remained low in
224 all cases (Fig. S2), suggesting that neither a low level of FruA nor a lack of D59 phosphorylation
225 causes the transcript levels to remain low in the *csgA* mutant. Rather, these results are
226 consistent with evidence suggesting that C-signaling regulates FruA activity by a mechanism
227 other than phosphorylation of its receiver domain (16, 18).
228
229 **Prior to FruA activation by C-signaling, unactivated FruA negatively regulates the late-acting**
230 **operons**
231 If C-signaling activates FruA and the activated FruA increases transcription of the late-acting
232 operons, then transcript levels are expected to be low in a *fruA* insertion mutant, as observed
233 for the *dev* operon (16). Instead, the *exoA*, *exoL*, and *nfsA* transcript levels of the *fruA* mutant
234 were greater than those of the WT strain at 18 h PS (Fig. 3), suggesting that FruA is a negative
235 regulator of the late-acting operons early in development. The *exoA* and *exoL* transcript levels
236 of the *fruA* mutant also exceeded those of the WT strain at 21 and 24 h. In contrast, the *fadI*
237 transcript level of the *fruA* mutant was less than that of the WT strain (Fig. 3D), consistent with
238 a model in which C-signaling activates FruA and the activated FruA increases *fadI* transcription.
239 Activated FruA may also increase *nfsA* transcription at 27 and 30 h, since the *nfsA* transcript
240 level of the *fruA* mutant was less than that of the WT strain at those times (Fig. 3C). The

241 average *exoA* transcript level of the *fruA* mutant was less than that of the WT strain at 30 h, but
242 this difference was due to one biological replicate of the WT strain with a much greater
243 transcript level than the other three replicates (Fig. 3A), so the evidence that activated FruA
244 increases *exoA* transcription at 30 h is weak. The average *exoL* transcript level of the *fruA*
245 mutant exceeded that of the WT strain at 27 and 30 h (Fig. 3B), providing no evidence that
246 activated FruA is necessary to increase *exoL* transcription.

247 Comparison of the *fruA* and *csgA* mutants suggests that FruA which has not been activated
248 by C-signaling (i.e., unactivated FruA) negatively regulates all four of the late-acting operons
249 early in development. The average transcript levels of the *fruA* mutant were greater than those
250 of the *csgA* mutant (except for the very low *fadI* transcript levels in both mutants at 27 and 30 h
251 PS) (Fig. 3). We also infer that negative regulation by unactivated FruA early in development of
252 the WT strain accounts for its relatively low *exoA* (Fig. 3A) and *exoL* (Fig. 3B) transcript levels at
253 18-24 h, and its low *nfsA* transcript level at 18 h (Fig. 3C), as compared with the *fruA* mutant.
254 The *fadI* transcript level of the WT strain was comparable to that of the *fruA* mutant at 18 h
255 (Fig. 3D), suggesting that positive regulation by activated FruA counteracts negative regulation
256 by unactivated FruA already by 18 h in this case.

257 Taken together, the effects of mutations in *fruA* and *csgA* on transcript levels suggest that
258 regulation of the late-acting operons during the period leading up to and including commitment
259 to spore formation depends on negative regulation by unactivated FruA, which in at least some
260 cases switches to positive regulation by C-signal-activated FruA.

261

262 **The *exoA*, *exoL*, and *nfsA* transcript levels of *mrpC* and *fruA* mutants differ**

263 MrpC appears to directly stimulate transcription from the *fruA* promoter (20). In agreement,
264 FruA was not detected in an *mrpC* in-frame deletion mutant at 18-30 h PS (16). Hence, the
265 *mrpC* mutant lacks both MrpC and FruA. To compare the loss of both transcription factors with
266 the loss of only FruA in terms of regulating the late-acting operons, we measured the transcript
267 levels of the *mrpC* mutant in parallel with those of the *fruA* mutant and the WT strain.
268 Strikingly, the *exoA*, *exoL*, and *nfsA* transcript levels of the *mrpC* and *fruA* mutants differed,
269 and in each case the pattern of effects was unique. The average *exoA* transcript level of the
270 *mrpC* mutant was greater than that of both the WT strain and the *fruA* mutant at all times (Fig.
271 5A, asterisks above error bars indicate $p < 0.05$ in Student's two-tailed *t*-tests comparing the
272 mutant to the WT strain at the same time point and asterisks above brackets likewise compare
273 the mutants). The comparison of mutants suggests that MrpC negatively regulates the *exoA*
274 transcript level independently of FruA (i.e., loss of both transcription factors increased the *exoA*
275 transcript level more than loss of only FruA). The *exoL* transcript level of the *mrpC* mutant
276 exceeded that of the WT strain at 18 and 24 h PS, and on average exceeded that of the *fruA*
277 mutant at 18 h, but on average was less than that of the *fruA* mutant at 24 and 30 h (Fig. 5B).
278 In this case, comparison of the mutants suggests that MrpC negatively regulates the transcript
279 level independently of FruA early in development, but that MrpC can positively regulate the
280 transcript level independently of FruA later in development. The *nfsA* and *fadI* transcript levels
281 of the WT strain increased at 30 h, but not those of the *mrpC* and *fruA* mutants (Fig. 5C and 5D),
282 nor of the *csgA* mutant (Fig. 3C and 3D), suggesting that C-signal-activated FruA positively
283 regulates the *nfsA* and *fadI* transcript levels late in development. However, earlier in
284 development at 18 h, the *nfsA* transcript level of the *fruA* mutant was greater than that of the

285 WT strain and the *mrpC* mutant (Fig. 5C), suggesting that MrpC positively regulates the
286 transcript level in the absence of FruA. In contrast, the *fadI* transcript level of both mutants
287 was less than that of the WT strain at 18 h (Fig. 5D), suggesting that both transcription factors
288 are required to positively regulate the transcript level. We conclude that each of the late-acting
289 operons is uniquely regulated by MrpC and FruA.

290 To determine whether the absence of MrpC and FruA in the *mrpC* mutant affects the
291 transcript degradation rates, we added rifampicin to inhibit transcription at 18 h PS and
292 determined the transcript levels at intervals thereafter. We chose 18 h for this analysis since
293 the *exoA* (Fig. 5A) and *exoL* (Fig. 5C) transcript levels were elevated in the *mrpC* mutant relative
294 to the WT strain at that time. The transcript degradation rates did not differ significantly
295 between the *mrpC* mutant and the WT strain (Fig. S3), suggesting that increased synthesis
296 (rather than decreased degradation) primarily accounts for the elevated *exoA* and *exoL*
297 transcript levels in the absence of MrpC and FruA.

298

299 **FruA can positively regulate *exoA*, *exoL*, and *nfsA* in the absence of MrpC**

300 To examine the effects of FruA in the absence of MrpC, we used the P_{van}-*fruA* fusion mentioned
301 previously (16) (Fig. S2) to produce FruA in the *mrpC* mutant. The inducer (vanillate) was added
302 during growth and at 0 h PS. At 6 h, the FruA level of the *mrpC* P_{van}-*fruA* mutant was about
303 threefold greater than that of the WT strain, but their FruA level was similar at 12 and 18 h (Fig.
304 S4A). Interestingly, the *mrpC* P_{van}-*fruA* mutant formed immature mounds by 12 h (Fig. S5),
305 although subsequent mound darkening was reduced compared to the WT strain (Fig. S6) and
306 spores were not detected (Table S1). Nevertheless, mound formation suggests that C-signaling

307 is activating FruA to some extent, since a complete block, as in *mrpC*, *fruA*, and *csgA* mutants,
308 results in no mound formation (16) (Fig. S5).

309 To determine the effects of FruA on regulation of the late-acting operons in the absence of
310 MrpC, we measured the transcript levels of the *mrpC* P_{van}-*fruA* mutant in parallel with those of
311 the *mrpC* and *fruA* mutants and the WT strain early in development. The *exoA* (Fig. 6A) and
312 *exoL* (Fig. 6B) transcript levels of the *mrpC* P_{van}-*fruA* mutant exceeded those of the WT strain at
313 6-18 h PS, and on average exceeded those of the *mrpC* and *fruA* mutants, except the *exoL*
314 transcript level of the *mrpC* mutant was similar to that of the *mrpC* P_{van}-*fruA* mutant at 18 h.
315 We conclude that FruA can positively regulate the *exoA* and *exoL* transcript levels in the
316 absence of MrpC. This regulation may involve C-signal-activated FruA since the *mrpC* P_{van}-*fruA*
317 mutant formed immature mounds (Fig. S5 and S6), whereas *mrpC*, *fruA*, and *csgA* mutants fail
318 to form mounds (16) (Fig. S5). The *nfsA* transcript level of the *mrpC* P_{van}-*fruA* strain exceeded
319 that of the WT strain at 6 h and the *mrpC* mutant at 6-12 h (Fig. 6C), also indicative of positive
320 regulation by FruA (perhaps activated FruA) in the absence of MrpC. On the other hand, the
321 *fadI* transcript level of the *mrpC* P_{van}-*fruA* strain was less than that of the WT strain (Fig. 6D), as
322 observed for the *mrpC*, *fruA*, and *csgA* mutants (Fig. 3D, 5D, and 6D), supporting that positive
323 regulation requires both MrpC and activated FruA.

324

325 **Nla6 positively regulates the transcript levels of the late-acting operons**

326 The Nla6 transcription factor appears to be a direct regulator of the *exoA-I* and *exoL-P* operons
327 since a protein with the *E. coli* maltose-binding protein (MBP) fused to the Nla6 DNA-binding
328 domain (DBD) bound to promoter region DNA fragments (50). A comparison of the *exoA* and

329 *exoL* transcript levels of a WT strain and an *nla6* insertion mutant suggested that Nla6 positively
330 regulates both during the first 8 h PS, and negatively regulates both at 24 h (50). We
331 constructed a new *nla6* insertion mutant and compared it with the one characterized
332 previously (50, 53). The new mutant is tetracycline-resistant (Tc^r) and the one described
333 previously is kanamycin-resistant (Km^r). Both mutants formed immature mounds by 12 h, but
334 failed to progress to more mature mounds with distinct, round edges by 18 h (Fig. S5). Later
335 during development, the Km^r *nla6* mutant mounds matured somewhat at 24-30 h, but failed to
336 darken by 36-48 h (Fig. S6). The Tc^r *nla6* mutant mounds did not mature until 36 h and also
337 failed to darken by 48 h. Spores were not detected for either mutant (Table S1).
338 The two *nla6* mutants were indistinguishable in terms of the molecular markers we tested.
339 Since our results showed that FruA and MrpC impact transcript levels of the late-acting operons
340 at 18 h PS (Fig. 3 and 5) and in some cases earlier during development (Fig. 6), we measured the
341 levels of FruA, MrpC, and transcripts from the late-acting operons for the *nla6* mutants in
342 parallel with the WT strain early in development. The FruA and MrpC protein levels of the *nla6*
343 mutants were similar to those of the WT strain at 6-18 h (Fig. S4). The *exoA*, *nfsA*, and *fadI*
344 transcript levels of the WT strain increased at 18 h, but those of the *nla6* mutants failed to
345 increase (Fig. 7), suggesting that Nla6 positively regulates the *exoA-I*, *nfsA-H*, and *fadIJ* operons.
346 The *exoL* transcript level of the WT strain did not increase at 18 h, but on average that of the
347 *nla6* mutants was less, suggesting that Nla6 also positively regulates the *exoL-P* operon.
348 Because the *exoA*, *exoL*, and *nfsA* transcript levels of the *mrpC* and/or *fruA* mutants exceeded
349 those of the WT strain early in development (Fig. 3, 5, and 6), we tried to construct *mrpC nla6*
350 and *fruA nla6* double mutants, but our efforts were unsuccessful, so we were unable to

351 determine whether positive regulation by Nla6 could account for the elevated transcript levels
352 in the *mrpC* and *fruA* mutants relative to the WT strain (see Discussion).
353
354 **Binding of the Nla6 DNA-binding domain, MrpC, and FruA differs at the promoter region of**
355 **each of the late-acting operons**
356 As a possible indication of direct regulation by Nla6, MrpC, and FruA, we tested for binding to a
357 DNA fragment upstream of the predicted start codon of the first gene in each of the late-acting
358 operons. Figure S7 shows features of each promoter region fragment based on previous work.
359 FruA and MrpC were shown to bind cooperatively to the *dev* promoter region fragment (28).
360 The FruA DBD was shown to bind to at least three sites in the *exoA-I* promoter region fragment
361 (49) and MBP-Nla6 DBD was also shown to bind, presumably *via* interaction with DNA
362 sequences similar to a half-site consensus sequence (50). MBP-Nla6 DBD was also shown to
363 bind to the *exoL-P* promoter region fragment (50). ChIP-seq analysis suggested that MrpC is
364 bound at a site upstream of *nfsA-H* at 18 h PS (27). Here, we used electrophoretic mobility shift
365 assays (EMSAs) to test for binding of purified MBP-Nla6 DBD, MrpC, and FruA separately, and in
366 combination because MrpC and FruA were shown previously to bind cooperatively to the *dev*,
367 *fmgA*, *fmgBC*, *fmgD*, and *fmgE* promoter regions (18, 28-31).
368 As expected (28), MrpC and FruA bound individually to the *dev* promoter region fragment
369 and the combination of MrpC and FruA exhibited greater binding (Fig. 8), suggestive of
370 cooperative binding. MrpC and FruA DBD also appeared to bind cooperatively (Fig. S8),
371 indicating the N-terminal domain of FruA was not required. Binding of MBP-Nla6 DBD was not

372 detected at 4 μM (Fig. 8), consistent with previous reports (19, 50), but binding was detected at
373 16 μM and increased at higher concentrations (Fig. S8).
374 The *fadIJ* promoter region fragment yielded results that were in some ways similar to those
375 for the *dev* fragment. MrpC and FruA bound individually to the *fadIJ* fragment, and the
376 combination of MrpC and FruA appeared to bind cooperatively, but with much less cooperative
377 binding than to the *dev* fragment (Fig. 8). The order of MrpC and FruA addition did not affect
378 cooperative binding to either fragment (Fig. 8 and S8). However, MrpC and FruA DBD did not
379 bind cooperatively to the *fadIJ* fragment, indicating a requirement for the FruA N-terminal
380 domain, in contrast to the *dev* fragment (Fig. S8). On the other hand, for both fragments, MBP-
381 Nla6 DBD binding was not detected at 4 μM and at that concentration did not affect binding of
382 MrpC or FruA (Fig. 8), but MBP-Nla6 DBD binding was detected at 16 μM and increased at
383 higher concentrations (Fig. S8). The apparent cooperative binding of MrpC and FruA to the
384 *fadIJ* fragment, together with our measurements of the *fadI* transcript level, support a similar
385 mechanism of developmental regulation of the *fadIJ* operon as proposed for the *dev* operon
386 (16, 28), the *fmg* genes (18, 29-31), and likely many other genes (27), in which C-signaling
387 activates FruA to bind DNA cooperatively with MrpC and increase transcription.
388 MBP-Nla6 DBD at 2 μM bound to the *exoA-I* promoter region fragment (Fig. 8), as expected
389 (50). FruA also bound (Fig. 8), as expected based on FruA DBD binding observed previously
390 (49). Strikingly, MBP-Nla6 DBD and FruA appeared to bind cooperatively and the order of
391 addition made no difference (Fig. 8 and S8). FruA DBD exhibited very little cooperative binding
392 with MBP-Nla6 DBD (Fig. S8), suggesting the N-terminal domain of FruA plays an important role.
393 Although MrpC appeared to negatively regulate the *exoA* transcript level independently of FruA

394 (Fig. 5A), binding of MrpC was not detected at 4 μM (Fig. 8) or at concentrations ranging up to
395 20 μM (Fig. 8S), and MrpC did not affect MBP-Nla6 DBD or FruA binding (Fig. 8). Taken
396 together, our results suggest that MrpC regulates *exoA* indirectly both independently of FruA
397 (Fig. 5A) and because MrpC is required for synthesis of FruA (16, 49), which together with Nla6
398 appears to directly regulate *exoA-I*.

399 We discovered that FruA binds to the *exoL-P* promoter region fragment (Fig. 8). Binding of
400 MBP-Nla6 DBD was not detected at 4 μM in the experiment shown in Figure 8, but was
401 detected at 4 μM in two other experiments (Fig. S8). Interestingly, MBP-Nla6 DBD and FruA
402 appeared to bind cooperatively and the order of addition made no difference, similar to our
403 results for the *exoA-I* promoter region fragment (Fig. 8 and S8). Both fragments also yielded
404 similar results in other experiments; FruA DBD exhibited very little cooperative binding with
405 MBP-Nla6 DBD (Fig. S8) and MrpC did not affect MBP-Nla6 DBD or FruA binding (Fig. 8).
406 However, the two fragments differed in terms of MrpC binding, which was not detected for the
407 *exoA-I* promoter region fragment at MrpC concentrations ranging up to 20 μM (Fig. 8S). In
408 contrast, for the *exoL-P* promoter region fragment, although binding of MrpC was not detected
409 at 4 μM in the experiment shown in Figure 8D, binding was detected at 4 μM and increased at
410 higher concentrations in another experiment (Fig. S8). Therefore, MrpC, as well as FruA and
411 Nla6, appear to directly regulate *exoL-P*, differentiating its regulation from that of *exoA-I* (see
412 Discussion).

413 We found that MBP-Nla6 DBD, MrpC, and FruA could each bind individually to the *nfsA-H*
414 promoter region fragment (Fig. 8). In combination with MBP-Nla6 DBD at 4 μM, individual
415 binding of MrpC was not detected and the intensity of the shifted complex increased at the

416 lagging edge (Fig. 8), suggestive of cooperative binding. In agreement, MBP-Nla6 DBD at 2 μM
417 appeared to bind cooperatively with MrpC, and the order of addition made little or no
418 difference (Fig. S8). We note that the large size of MBP-Nla6 DBD and the DNA fragment likely
419 explain the small difference in migration of the putative MBP-Nla6 DBD/MrpC/DNA complex
420 compared to the MBP-Nla6 DBD/DNA complex. Like MrpC, FruA appeared to bind
421 cooperatively with MBP-Nla6 DBD (Fig. 8 and S8). In the mixtures with MBP-Nla6 DBD,
422 individual binding of FruA was detected, suggestive of less cooperativity than in the case of
423 MrpC. FruA DBD did not appear to bind cooperatively MBP-Nla6 DBD, and FruA did not appear
424 to bind cooperatively with MrpC (Fig. S8). We conclude that MBP-Nla6 DBD, MrpC, and FruA
425 appear to directly regulate *nfsA-H* and we note that the apparent cooperative binding of MBP-
426 Nla6 DBD and MrpC to the *nfsA-H* promoter region fragment distinguishes it from the *exoA-I*
427 and *exoL-P* fragments we tested.
428
429 **DevI negatively regulates the transcript levels of the late-acting operons**
430 Reporter activity from fusions to *exoC* (48) and *nfsA* (44) was reduced in a *devRS* insertion
431 mutant compared with a WT strain during development. The *exoA* transcript level was also
432 reduced in a *devS* in-frame deletion mutant compared with a WT strain during development
433 (41). To further investigate the effects of mutations in components of the *dev* CRISPR-Cas
434 system on regulation of the late-acting operons, we measured transcript levels in *devI* and *devS*
435 in-frame deletion mutants. Sporulation occurs about 6 h earlier than normal in the *devI* mutant
436 (16, 41), suggesting that DevI delays sporulation of the WT strain. Sporulation is severely

437 impaired in the *devS* mutant (16, 39) due to loss of negative autoregulation of *dev* transcription
438 and resulting overproduction of DevI, which strongly inhibits sporulation (40).
439 We found that the *exoA*, *exoL*, *nfsA*, and *fadI* transcript levels remain low in the *devS*
440 mutant at 18-30 h PS (Fig. 9). We infer that DevI overproduction in the *devS* mutant inhibits
441 accumulation of transcripts from the late-acting operons. Although Student's two-tailed *t*-tests
442 rarely yielded $p < 0.05$ comparing transcript levels in the *devS* mutant with the WT strain at the
443 corresponding time PS, this was due to the large variation between biological replicates of the
444 WT strain. We emphasize that transcript levels were low in all biological replicates of the *devS*
445 mutant at all times PS.
446 The average transcript level was greater in the *devI* mutant than the WT strain, except the
447 *nfsA* transcript levels were equal at 30 h PS (Fig. 9). These results are consistent with the notion
448 that DevI inhibits accumulation of transcripts from the late-acting operons. Here again,
449 Student's two-tailed *t*-tests rarely yielded $p < 0.05$, but in this case there was large variation
450 between biological replicates of both the *devI* mutant and the WT strain. Even so, taken
451 together, the measurements of transcript levels in the *devI* and *devS* mutants support that DevI
452 is a negative regulator of the late-acting operons.
453
454 **Discussion**
455 Our results reveal complex regulation of genes involved in spore metabolism and spore coat
456 biogenesis during *M. xanthus* development (Fig. 10). Prior to its activation by C-signaling, FruA
457 appears to negatively regulate transcription of the late-acting *fadIJ*, *nfsA-H*, *exoA-I*, and *exoL-P*
458 operons (red line with barred end), then C-signal-activated FruA (designated FruA*) appears to

459 positively regulate transcription of these operons during spore formation (green arrow).
460 However, each operon is unique in terms of the strength of negative and positive regulation by
461 FruA. Moreover, MrpC differentially regulates each operon, exerting negative and/or positive
462 effects independently of FruA/FruA* or cooperatively. The negative effect of MrpC on *exoA-I*
463 appears to be indirect since binding to the promoter region *in vitro* was not detected (dashed
464 red line with barred end), but the effects of MrpC on the other three operons may be direct
465 since MrpC binds to their promoter regions (red line with barred end to *exoL-P* early, green
466 arrow to *nfsA-H* early, and green arrows to *exoL-P* and *fadIJ* late). FruA binds to all four
467 promoter regions. Unusually for bacterial genes, a third transcription factor, Nla6, also binds to
468 the promoter regions. Interestingly, Nla6 bound cooperatively with FruA and with MrpC to the
469 *nfsA-H* promoter region, but Nla6 bound cooperatively only with FruA to the *exoA-I* and *exoL-P*
470 promoter regions. Nla6 appears to positively regulate all four operons early in development
471 (green arrows). The positive effect of Nla6 on *fadIJ* may be indirect (dashed green arrow) since
472 binding to the promoter region required a high concentration of Nla6. DevI negatively
473 regulates transcript levels from all four operons (dashed red line with barred end), providing
474 new insight into the regulation of *M. xanthus* development by a CRISPR-Cas system. We
475 conclude that three transcription factors and a CRISPR-Cas component regulate the late-acting
476 operons and we propose this ensures that spore resistance and surface characteristics meet
477 environmental demands.
478
479 **New insights into the functions of the late-acting operons**

480 Our results show that mutations in *exoC*, *nfsA-H*, and *exoL* do not prevent the initial cellular
481 shape change associated with sporulation (Fig. S1B), but do impact the formation of sonication-
482 resistant spores beginning at 27 h PS (Fig. 2). Previously, these mutants were examined for
483 starvation-induced spore formation at 120 h (45, 50, 51). Our findings indicate a much earlier
484 role of the ExoA-I, NfsA-H, and ExoL-P proteins during starvation-induced sporulation than
485 established previously. Glutaraldehyde fixation of cells followed by brief sonication allowed us
486 to visualize and enumerate cells that appeared to be transitioning from rods to spores in
487 samples of the starved mutants (Fig. S1B). These TCs likely resemble cells of *exo* and *nfs*
488 mutants that fail to complete morphogenesis upon chemical induction of sporulation in liquid
489 culture (45, 46, 51).

490 The WT strain may exhibit a higher percentage of TCs than the *fadI* mutant (Fig. S1B)
491 because the mutant makes more sonication-resistant spores (Fig. 2). The *fadI* insertion mutant
492 presumably has a reduced rate of fatty acid β-oxidation, as appeared to be the case for a *fadIJ*
493 (*MXAN5372-MXAN5371*) deletion mutant (42), so perhaps altered metabolism enhanced
494 formation of sonication-resistant spores by the *fadI* mutant at 27-48 h (Fig. 2), albeit not
495 mature spores at 72 h (Table S1).

496 The *nfsA-H* mutant made about twofold less sonication-resistant spores than the WT strain,
497 whereas the *exoC* and *exoL* mutants made less than the detection limit (Fig. 2). For these three
498 mutants, the lower percentage of TCs as compared with the WT strain at 24 and 27 h (Fig. S1B)
499 may reflect reduced ability to initiate and/or maintain the cellular shape change associated with
500 sporulation. Upon chemical induction of sporulation, *exoC*, *nfsA-H*, and *exoL* mutants appeared
501 to initiate the transition from rods to spores, but then revert into rods or form branched rods,

502 ovoid-shaped cells, or large spheres (45, 46, 51). Given the evidence that Exo and Nfs proteins
503 function in spore coat polysaccharide export (45, 46, 51, 54) and assembly (45-47), respectively,
504 our results suggest that defective spore coat biogenesis of the *exoC*, *nfsA-H*, and *exoL* mutants
505 reduces their ability to maintain cellular shape change as early as 24 h (Fig. S1B) and blocks or
506 reduces their ability to form sonication-resistant spores by 27 h (Fig. 2) and mature spores by
507 72 h (Table S1) (Fig. 10).

508 The milder sporulation defect of the *nfsA-H* mutant compared with the *exoC* and *exoL*
509 mutants (Fig. 2, Table S1) is consistent with previous reports (45, 50, 51). The *exoC* mutant fails
510 to export spore coat polysaccharide, whereas the *nfsA-H* mutant appears to export it, but fails
511 to assemble it properly, producing an amorphous, unstructured spore coat that nevertheless
512 appears to provide some heat- and sonication-resistance (45). The Nfs machinery shortens the
513 polysaccharide chains, decreases their surface abundance, and with the help of the AglQRS
514 motor assembles the compact, rigid, fully stress-resistant coat of mature spores (46, 47).

515

516 **Unactivated FruA negatively regulates transcription of the late-acting operons early in**
517 **development**

518 Our measurements of transcript levels in a *fruA* mutant indicate that FruA negatively regulates
519 the late-acting operons. The *fruA* mutation elevated the average *exoA*, *exoL*, and *nfsA*
520 transcript levels 17-, 57-, and 4-fold, respectively, relative to the WT strain at 18 h PS (Fig. 3).
521 The *fruA* mutation did not elevate the average *fadI* transcript level compared to the WT strain,
522 but the *fadI* transcript level was 8-fold greater in the *fruA* mutant than in the *csgA* mutant (p =
523 0.002 in a Student's two-tailed t-test). Since FruA* appears to be present by 18 h in the WT

524 strain (16), positive regulation by FruA* likely counteracts negative regulation by unactivated
525 FruA. However, in the *csgA* mutant, only unactivated FruA is present, resulting in a very low
526 *fadI* transcript level, as well as very low transcript levels from the other late-acting operons (Fig.
527 3). Neither *mrpC* nor *csgA* mutations altered the degradation rates of transcripts from the late-
528 acting operons (Fig. 4 and S3). Therefore, since unactivated FruA is absent from the *mrpC*
529 mutant and present in the *csgA* mutant (16), we conclude that unactivated FruA regulates the
530 synthesis rather than the degradation of transcripts from the late-acting operons at 18 h, which
531 we consider early in development since mounds (Fig. 1) but not spores have formed (Fig. 2).
532 This negative regulation of transcription by unactivated FruA is summarized in Figure 10 by a
533 red line with barred end that extends from FruA toward a gray box including all four late-acting
534 operons.

535 Our results agree qualitatively with two prior reports of negative regulation by FruA early in
536 development. Expression of a reporter fused to the *nfsA-H* promoter region was elevated 2-
537 fold in a *fruA* mutant compared with a WT strain at 12-18 h PS (44). We observed that the
538 average *nfsA* transcript level was consistently elevated at least 4-fold in a *fruA* mutant
539 compared with a WT strain at 18 h (Fig. 3C, 5C, and 6C), but elevated in only one of three
540 replicates at 12 h (Fig. 6C). The difference in the strength of regulation between the studies
541 may be due to differences in the strains and/or the methods. The difference between
542 replicates at 12 h in our study reflects experimental variation in the timing of induction of *nfsA-*
543 *H* transcription.

544 While our work was in progress, transcriptomic analysis of a *fruA* mutant compared with a
545 WT strain identified > 1000 genes that were negatively regulated by FruA at one or more time

546 points during the first 24 h of development (55). The transcript levels of all genes in the late-
547 acting operons were elevated in a *fruA* mutant relative to a WT strain at 12 h (Table S2). In our
548 study, the transcript levels were not elevated in the *fruA* mutant relative to the WT strain at 12
549 h (Fig. 6), except the one replicate for *nfsA* mentioned above (Fig. 6C). The strength of
550 regulation also differed between the studies (compare Fig. 3 and Table S2). Interestingly, the
551 fold increase in transcript levels varied greatly for different genes in the *exoA-I* and *exoL-P*
552 operons (Table S2), perhaps reflecting differential regulation. We measured transcript levels of
553 the first gene in each operon, but even focusing on the results for the first gene in each operon
554 reveals large differences between the studies in the strength of regulation (i.e., 25-, 11-, and
555 15-fold differences for *exoA*, *exoL*, and *nfsA*, respectively, between the 12-h values in Table S2
556 and the 18-h values mentioned above for Fig. 3). In support of our conclusion that regulation of
557 *fadIJ* switches from negative by unactivated FruA to positive by FruA*, *fadIJ* transcript levels
558 were elevated 2-fold in a *fruA* mutant compared with a WT at 12 h, but elevated 4-fold in the
559 WT strain compared with the *fruA* mutant at 24 h (Table S2). Importantly, we note that *exoA-I*,
560 *exoL-P*, and *nfsA-H* transcript levels decline sharply in the *fruA* mutant relative to the WT strain
561 between 12 and 24 h, which may be a signature for late-acting genes in the data of McLoon *et*
562 *al.* (55).
563

564 **MrpC and Nla6 contribute to differential regulation of the late-acting operons**

565 The switch from negative regulation of *fadIJ* transcription by unactivated FruA to positive
566 regulation by FruA* requires MrpC (Fig. 10) since the *fadI* transcript level did not increase in the
567 *mrpC* mutant (Fig. 5D and 6D) or the *mrpC* mutant engineered to express FruA from a vanillate-

568 inducible promoter (Fig. 6D). MrpC and FruA bound individually and with weak cooperativity to
569 the *fadIJ* promoter region *in vitro* (Fig. 8 and S8). Cooperative binding of MrpC and FruA *in vitro*
570 has been correlated with positive regulation *in vivo* for *dev* (28) and *fmg* (16, 18, 29-31) genes,
571 leading to a model in which MrpC and FruA* bind cooperatively upstream of the promoter and
572 increase transcription. Positive regulation of *fadIJ* transcription appears to fit this model since
573 expression from a *fadI* reporter fusion was twofold lower in *mrpC*, *fruA*, and *csgA* mutants than
574 in a WT strain at 18 and 24 h PS (42), and matches to the consensus sequences for MrpC and
575 FruA binding are present upstream of the promoter (Fig. S9). In particular, the matches to the
576 consensus sequences for MrpC and FruA binding centered at -96 and -69.5, respectively, are
577 well-positioned to explain cooperative binding of MrpC and FruA* that could increase
578 transcription. Bullock *et al.* did not observe elevated expression in a *fruA* mutant relative to the
579 other strains (i.e., evidence for negative regulation by unactivated FruA), perhaps due to
580 differences in the strains and/or the methods. The negative regulation of *fadIJ* by unactivated
581 FruA that both we and McLoon *et al.* observed (as explained above) distinguishes the regulation
582 of *fadIJ* transcription from that of *dev* (Fig. 10) and *fmg* genes since neither reporter fusion
583 expression nor transcript levels of *dev* (15, 16, 55, 56) and *fmg* (29, 30, 55, 57, 58) genes are
584 elevated in *fruA* mutants (Table S3). Perhaps unactivated FruA binds to the putative site
585 centered at -69.5 and/or other putative FruA-binding sites upstream of the *fadIJ* promoter (Fig.
586 S9), preventing a low level of transcription that can occur in the absence of FruA (Fig. 3D, 5D,
587 and 6D) (55) (Table S2) but not in the absence of MrpC (Fig. 5D and 6D).
588 Regulation of the *nfsA-H* operon by MrpC was unique among the late-acting operons since
589 the *nfsA* transcript level was much greater in the *fruA* mutant than in the WT strain or the *mrpC*

590 mutant at 18 h PS (Fig. 5C and 6C). Since the MrpC level in the *fruA* mutant is similar to that in
591 the WT strain (16) and both MrpC and FruA bind independently (without cooperativity) to the
592 *nfsA-H* promoter region (Fig. 8 and S8), we infer that MrpC can directly increase *nfsA-H*
593 transcription but that unactivated FruA directly opposes an increase early in development (Fig.
594 10). Later (e.g., at 27 and 30 h), FruA* appears to be required to increase *nfsA-H* transcription
595 (Fig. 3C) and can do so without MrpC (Fig. 6C, note the *y*-axis scale is different than in Fig. 3C)
596 (Fig. 10). The best match to the consensus sequence for MrpC binding is centered at -29 in the
597 *nfsA-H* promoter region (Fig. S9), consistent with the location of an MrpC-binding site identified
598 by ChIP-seq analysis (27) (Fig. S7). The best match to the consensus sequence for FruA binding
599 is centered at -82.5. Binding of MrpC and FruA to sites centered at -29 and -82.5, respectively,
600 may explain the lack of cooperative binding *in vitro* (Fig. 8 and S8), but how unactivated FruA
601 bound to the upstream site would oppose an increase in transcription caused by MrpC bound
602 to the downstream site early in development is unclear (Fig. 10). We note that upstream of the
603 putative FruA-binding site centered at -82.5 there are several overlapping sequences that
604 match the FruA and MrpC consensus sequences except at one or two positions, respectively
605 (Fig. S9). If those putative MrpC-binding sites increase transcription directly or indirectly (e.g.,
606 by aiding recruitment of MrpC to the site centered at -29), then binding of unactivated FruA to
607 overlapping sites could oppose an increase in transcription early in development (Fig. 10).
608 Alternatively, unactivated FruA bound to any of three putative upstream sites may oppose an
609 increase in transcription mediated by Nla6. MBP-Nla6 DBD bound cooperatively with FruA to
610 the *nfsA-H* promoter region (Fig. 8 and S8), and a sequence matching the Nla6 half-site
611 consensus sequence (50) except at one position is centered at -100.5 (Fig. S9) and may be

612 involved in the cooperative binding. Testing these hypotheses and elucidating how FruA*
613 increases transcription later in development will require much more work. MBP-Nla6 DBD also
614 bound cooperatively with MrpC to the *nfsA-H* promoter region (Fig. 8 and S8), and a putative
615 Nla6 half-site centered at -42.5 appears to be well-positioned for cooperative binding, but it is
616 unclear whether this affects transcription.

617 Regulation of the *exoA-I* and *exoL-P* operons by MrpC was different from that of the *nfsA-H*
618 and *fadIJ* operons since the average *exoA* and *exoL* transcript levels were greater in the *mrpC*
619 mutant than in the WT strain or the *fruA* mutant at 18 h PS (Fig. 5AB and 6AB). These results
620 suggest that MrpC contributes to negative regulation of the *exoA-I* and *exoL-P* operons both
621 independently of FruA and because MrpC is required for synthesis of unactivated FruA (16, 49),
622 which negatively regulates the operons early in development (Fig. 10).

623 Negative regulation of *exoA-I* by MrpC independently of FruA appears to be indirect (dashed
624 red line with barred end in Fig. 10) since binding of MrpC to the promoter region *in vitro* was
625 not detected (Fig. S8). Negative regulation of *exoA-I* by unactivated FruA early in development
626 may involve overlapping FruA- and Nla6-binding half-sites (Fig. S7 and S9). The FruA-binding
627 site depicted as centered at -75.5 in Figure S7 based on DNase I footprinting (49), encompasses
628 two matches to the FruA consensus binding sequence, and the match centered at -83 overlaps
629 a putative Nla6-binding half-site centered at -88.5 (Fig. S9). A putative FruA-binding site
630 centered at -42 overlaps two putative Nla6-binding half-sites. FruA and MBP-Nla6 DBD bound
631 cooperatively to the *exoA-I* promoter region (Fig. 8 and S8). We propose that unactivated FruA
632 interferes with transcriptional activation by Nla6 early in development. The very low *exoA*
633 transcript level in a *csgA* mutant (Fig. 3A) despite a similar transcript degradation rate as the

634 WT strain (Fig. 4AE), and our finding that FruA expression increases the transcript level in the
635 absence of MrpC (Fig. 6A), suggest that FruA* increases *exoA-I* transcription later in
636 development (Fig. 10). In contrast, Nla6 negatively regulates the *exoA* transcript level twofold
637 at 24 h PS (50) (Fig. 10). Perhaps the concentration of Nla6 decreases during development
638 and/or C-signal-dependent formation of FruA* increases its binding to DNA or changes its
639 cooperative binding with Nla6, allowing FruA* to activate *exoA-I* transcription.
640 Negative regulation of *exoL-P* by MrpC independently of FruA may involve overlap of an
641 MrpC-binding site with an Nla6-binding half-site. The best match to the consensus sequence
642 for MrpC binding is centered at -99 and partially overlaps a putative Nla6-binding half-site
643 centered at -89.5 (Fig. S7 and S9). Both MrpC and MBP-Nla6 DBD bound weakly to the *exoL-P*
644 promoter region and the two proteins did not bind cooperatively (Fig. 8 and 8S). In this case,
645 MrpC may compete with Nla6 for binding and thus interfere with transcriptional activation by
646 Nla6 early in development (Fig. 10). In contrast, negative regulation by unactivated FruA may
647 involve cooperative binding with Nla6, as proposed for *exoI-A* and possibly *nfsA-H* transcription,
648 since FruA and MBP-Nla6 DBD bound cooperatively to the *exoL-P* promoter region (Fig. 8 and
649 S8). Putative Nla6-binding half-sites centered at -115.5 and -46.5 are adjacent to putative FruA-
650 binding sites centered at -130 and -62, respectively (Fig. S7 and S9), which may allow
651 cooperative binding that interferes with transcriptional activation by Nla6 early in development
652 (Fig. 10). For similar reasons as mentioned above for the *exoA* transcript, our results for the
653 *exoL* transcript (Fig. 3B, 4BE, and 6B) suggest that FruA* increases *exoL-P* transcription later in
654 development, and previous work showed that Nla6 negatively regulates the *exoL* transcript
655 level twofold at 24 h PS (50) (Fig. 10). Therefore, similar mechanisms may allow FruA* to

656 activate *exoL-P* and *exoA-I* transcription. A striking difference between regulation of *exoL-P* and
657 *exoA-I* late in development is that MrpC positively regulates the *exoL-P* transcript level
658 independently of FruA (Fig. 5AB and 10). Consistent with MrpC acting independently of FruA,
659 the two proteins did not appear to bind cooperatively to the *exoL-P* promoter region (Fig. 8),
660 perhaps because the distance between putative binding sites is too great (Fig. S9).
661 To summarize, null mutations in *mrpC* and *fruA* uniquely affect the transcript levels from
662 each of the late-acting operons. The observed differential regulation may be explained in part
663 by the positions and affinities of binding sites for MrpC, FruA, and Nla6 in each promoter
664 region. Cooperative binding also appears to be involved, exerting positive or negative effects.
665 The C-signal-dependent switch from negative regulation by unactivated FruA early in
666 development to positive regulation by FruA* later also plays an important role. This process, as
667 well as potential changes in the levels and activities of MrpC and Nla6, will require further
668 investigation in order to better understand the differential regulation of each late-acting
669 operon.
670
671 **DevI is a negative regulator of the late-acting operons**
672 Our results confirm and extend the role of DevI as a negative regulator of late-acting operons
673 during development. Previous studies implicated DevRS proteins in positive regulation of *exoA-*
674 *I* (48) and *nfsA-H* (44). Subsequently, DevTRS proteins were shown to negatively autoregulate
675 the *dev* operon, which codes for DevI, a 40-residue protein that strongly inhibits sporulation
676 when overproduced (40) and delays sporulation by about 6 h when produced at the normal
677 level (16, 41). As expected, the *exoA* transcript level was very low in a *devS* null mutant (41).

678 We confirmed that result and also showed that the *exoL*, *nfsA*, and *fadI* transcript levels are
679 very low in the *devS* mutant at 18-30 h PS (Fig. 9). We also found that transcript levels from the
680 late-acting operons were slightly greater on average in a *devI* null mutant than in the WT strain,
681 supporting our conclusion that DevI is a negative regulator of the late-acting operons late in
682 development (Fig. 10). However, the mechanism of negative regulation by DevI is unknown.
683 The *devS* mutant failed to undergo normal cellular shape change as determined by light
684 microscopic observation (41), presumably because DevI overproduction inhibits cellular shape
685 change (Fig. 10). This could be a cumulative effect of failure to express the late-acting operons,
686 given that mutations in the individual operons did not prevent cellular shape change (Fig. S1B).
687 Alternatively, one or more other genes subject to negative regulation by DevI overproduction
688 may account for the failure of the *devS* mutant to undergo normal cellular shape change. The
689 method devised in this work to quantify TCs after glutaraldehyde fixation and brief sonication,
690 and the recently reported *in situ* confocal microscopy approaches (33), would provide more
691 sensitive measures of cellular shape change by the *devS* mutant than the light microscopy
692 method (41).
693
694 **Combinatorial control of genes involved in spore formation**
695 Eukaryotic-like signaling and gene regulation has been known in *M. xanthus* for decades (59,
696 60). More recently, combinatorial control, a common theme in eukaryotic gene regulatory
697 networks (61), emerged from studies of *M. xanthus* gene regulation (4). Combinatorial control
698 allows signal integration by utilizing two or more signal-responsive transcription factors to
699 directly regulate the same gene. During *M. xanthus* development, the cascade of enhancer-

700 binding proteins (EBPs) that includes Nla6 has several instances of combinatorial control by two
701 EBPs (4, 19, 62). MrpC and FruA appear to combinatorially control the *dev* operon (16, 28), the
702 *fmg* genes (18, 29-31), and likely many other genes (27) by binding cooperatively to the
703 promoter regions. MrpC and FruA also bind cooperatively to the promoter region of the *fadIJ*
704 operon (Fig. 8 and S8) involved in spore fatty acid metabolism (42). Combinatorial control by
705 cooperative binding of MrpC and FruA may ensure that only starving rods aligned in mounds
706 commit to spore formation (4, 18, 25, 33, 34).
707 Importantly, combinatorial control of the *nfsA-H*, *exoA-I*, and *exoL-P* operons involved in
708 spore coat biogenesis does not appear to involve cooperative binding of MrpC and FruA (Fig. 8
709 and S8). Rather, MBP-Nla6 DBD bound cooperatively with FruA to all three promoter regions
710 and with MrpC only to the *nfsA-H* promoter region. Based on our current understanding of the
711 signaling and gene regulatory network, Nla6 indirectly responds to starvation and cell density-
712 dependent A-signaling early in development (4, 19). It is unclear whether Nla6 responds to
713 other signals later in development. A high cell density near the radial center of early nascent
714 fruiting bodies correlates with a high spore proportion later (33), so perhaps A-signaling plays a
715 role in early spatial patterning of subsequent sporulation *via* Nla6-mediated positive regulation
716 (Fig. 10). Alternatively or in addition, negative regulation by Nla6 of *exoA-I* and *exoL-P* later in
717 development may prevent premature synthesis, export, and modification of the spore coat
718 polysaccharide. Combinatorial control of *exoL-P* also appears to involve MrpC binding
719 separately (i.e., without cooperativity) (Fig. 8) and regulating negatively early in development
720 and positively later (Fig. 10).

721 We propose that combinatorial control of the late-acting operons by signal-responsive
722 transcription factors allows proper temporal and spatial expression of genes involved in spore
723 metabolism and coat biogenesis in order to produce spores that are densely packed in fruiting
724 bodies and suited to withstand environmental insults. Several transcription factors likewise
725 positively and negatively fine-tune the expression of hundreds of genes during *Bacillus subtilis*
726 endospore formation (63-65), ensuring that the resulting spores are endowed with resistance
727 and surface properties tailored for their environment (66-68). In *M. xanthus*, the Dev proteins
728 of a CRISPR-Cas system provide yet another layer of regulation of the late-acting operons (Fig. 9
729 and 10), and one signal to which this system responds may be bacteriophage infection (39).
730 In summary, our investigation uncovered complex regulation of genes involved in spore
731 metabolism and spore coat biogenesis by three transcription factors and a CRISPR-Cas
732 component during *M. xanthus* development. Further elucidating the signals to which Nla6,
733 MrpC, and FruA respond, understanding how these transcription factors interact at promoter
734 regions with many potential binding sites (Fig. S9), and elucidating how DevI inhibits the cellular
735 shape change associated with sporulation, are important goals for the future.
736

737 **Material and Methods**

738 ***Bacterial strains, plasmids and primers***

739 The strains, plasmids and primers used in this study are listed in Table S4.
740 *M. xanthus* strain MSS2 with P_{van}-*fruA* integrated ectopically was constructed by
741 electroporating (69) pSS10 into strain DK1622, selecting transformants on CTT agar (1%
742 Casitone, 10 mM Tris-HCl [pH 8.0], 1 mM KH_2PO_4-K_2HPO_4, 8 mM $MgSO_4$ [final pH 7.6] solidified

743 with 1.5% agar) containing 15 μg/mL tetracycline (70), and verification by colony PCR using
744 primers pMR3691 MCS G-F and pMR3691 MCS G-R.
745 *M. xanthus* strain MSS10 with a plasmid insertion mutation in *nla6* was constructed by
746 electroporating pSS11 into strain DK1622, selecting transformants on CTT agar containing
747 tetracycline (15 μg/mL), and verification by colony PCR using primers PMR3487 Rev, Nla6 Fwd4,
748 and Nla6 Fwd5. To construct pSS11, primers Nla6 Fwd and Nla6 Rev were used to generate a
749 PCR product using chromosomal DNA from *M. xanthus* strain DK1622 as a template. The
750 product was combined with DNA amplified from pMR3487 using primers PMR3487G Fwd and
751 PMR3487G Rev primers, and a Gibson assembly reaction was used to enzymatically join the
752 overlapping DNA fragments (71). The reaction mixture was transformed into *E. coli* strain
753 DH5α, transformants were selected at 37°C on Luria-Bertani (LB) (72) 1.5% agar containing 15
754 μg/mL tetracycline, and the cloned DNA sequence was verified using primers 3487 seq Fwd1,
755 3487 seq Fwd2, 3487 seq Fwd3, 3487 seq Fwd4, and 3487 seq Fwd5.
756 To provide a DNA template for amplification of the *nfsA-H* promoter region, pSS14 was
757 constructed as follows. Primers Nfs -290G and Nfs +83G were used to generate a PCR product
758 using chromosomal DNA from *M. xanthus* strain DK1622 as a template. The product was
759 combined with DNA amplified from pMR3487, the overlapping DNA fragments were joined
760 using a Gibson assembly reaction, the reaction mixture was transformed into *E. coli* strain
761 DH5α, transformants were selected, and the cloned DNA sequence was verified as described
762 above for pSS11.
763 To express MBP-Nla6 DBD for purification, primers Nla DBD For and Nla DBD Rev were used
764 to generate a PCR product using *nla6* DNA as a template. The PCR product was digest with *Sbf*I

765 and ligated to *Xmn*I-*Sbf*I-digested pMAL-c5x (NEB), resulting in pMAL-c5x/MBP-ΔCNla6 DBD,
766 which lacked a CG bp at the beginning of the Nla6 DBD-encoding segment. The missing CG bp
767 was added by performing site-directed mutagenesis using the QuikChange strategy (Stratagene)
768 with primers MBP-Nla6 add C fwd and MBP-Nla6 add C rev, resulting in pMAL-c5x/MBP-Nla6
769 DBD, and the DNA sequence was verified using primer mbp fwd colpcr.
770
771 ***Growth and development of* M. xanthus**
772 Strains of *M. xanthus* were grown at 32°C in CTTYE liquid medium (CTT medium with 0.2% yeast
773 extract) with shaking at 350 rpm. CTT agar was used for growth on solid medium and was
774 supplemented with 40 μg/mL of kanamycin sulfate or 15 μg/mL of tetracycline as required.
775 Fruiting body development under submerged culture conditions was performed using MC7 (10
776 mM morpholinepropanesulfonic acid [MOPS; pH 7.0], 1 mM $CaCl_2$) as the starvation buffer as
777 described previously (25). Briefly, cells in the mid-exponential phase of growth were collected
778 by centrifugation, the supernatant was removed, and the cells were resuspended in MC7 buffer
779 at a density of approximately 1,000 Klett units. A 96-μL sample (designated T_0) was removed
780 and 4 μL of glutaraldehyde was added from a 50% stock solution to achieve a 2% final
781 concentration. The sample was stored at 4°C for at least 24 h in order to fix the cells for later
782 quantification of total cells as described below. For each developmental sample, 1.5 mL of the
783 1,000-Klett-unit cell suspension plus 10.5 mL of MC7 buffer was added to an 8.5-cm-diameter
784 plastic petri plate. Upon incubation at 32°C, cells adhere to the bottom of the plate and
785 undergo development. At the indicated times, developing populations were photographed
786 using a Leica Wild M8 microscope equipped with an Olympus E-620 digital camera.

787

788 ***Sample collection***

789 At the indicated times PS, the MC7 buffer overlay was replaced with 5 mL of fresh MC7 buffer
790 or 5 mL of MC7 buffer containing 50 μg/mL of rifampicin to inhibit transcription for
791 measurement of transcript degradation rates. Developing cells were scraped from the bottom
792 of the plates, the entire contents were collected in a 15-mL centrifuge tube, and samples were
793 mixed thoroughly as described previously (16). A 96-μL sample was removed, glutaraldehyde
794 was added, and the sample was stored as described above for the T_0 sample, fixing the cells for
795 quantification of total cells as described below. A 400 μL sample was removed and stored at -
796 20°C for measurement of sonication-resistant spores as described below. For the experiments
797 shown in Figures 7 and S4, a 100 μl sample was removed and added to an equal volume of 2×
798 sample buffer (0.125 M Tris-HCl [pH 6.8], 20% glycerol, 4% sodium dodecyl sulfate [SDS], 0.2%
799 bromophenol blue, 0.2 M dithiothreitol), boiled for 5 min, and stored at -20°C for immunoblot
800 analysis. Immediately after collecting the samples just described, the rest of the 1,000-Klett-
801 unit cell suspension was mixed with 0.5 mL of RNase stop solution (5% phenol [pH < 7] in
802 ethanol), followed by rapid cooling in liquid nitrogen until almost frozen, centrifugation at 8,700
803 × *g* for 10 min at 4°C, removal of the supernatant, freezing of the cell pellet in liquid nitrogen,
804 and storage at -80°C until RNA extraction.

805

806 ***Quantification of total cells, transitioning cells, and sonication-resistant spores***

807 The total number of cells, including rods, elliptical TCs, and round spores, was determined using
808 the glutaraldehyde-fixed samples collected as described above. Each sample was thawed and

809 mixed by vortexing and pipetting, diluted with MC7 buffer, sonicated for 10 s, and then all cells
810 were counted microscopically as described previously (16), except noting the number of cells
811 that were elliptical or round. The number of sonication-resistant spores in the 400-μL samples
812 collected as described above was quantified as described previously (25). These samples were
813 not glutaraldehyde-fixed and were sonicated for 10 s intervals three times with cooling on ice in
814 between, leaving only round spores (i.e., neither rods nor elliptical TCs were observed). The
815 total cell number minus the number of sonication-resistant spores was designated the number
816 of sonication-sensitive cells (consisting primarily of rods and a small percentage of TCs) and was
817 expressed as a percentage of the total cell number in the corresponding T_0 sample (consisting
818 only of rods). The number of cells that were elliptical or round in the glutaraldehyde-fixed
819 sample minus the number of sonication-resistant spores in the corresponding sample that was
820 not glutaraldehyde-fixed, was designated the number of TCs and was also expressed as a
821 percentage of the total cell number in the corresponding T_0 sample.
822
823 ***RNA extraction and analysis***
824 RNA was extracted using the hot-phenol method, followed by digestion with DNase I (Roche) as
825 described previously (23). The RNA (1 μg) was then subjected to cDNA synthesis using
826 Superscript III reverse transcriptase (InVitrogen) and random primers (Promega), as instructed
827 by the manufacturers. In parallel, RNA (1 μg) was subjected to cDNA synthesis reaction
828 conditions without Superscript III reverse transcriptase, as a control. One μl of cDNA at the
829 appropriate dilution (as determined empirically) and 20 pmol of each primer were subjected to
830 qPCR in a 25 μl reaction using 2× reaction buffer as described previously (16). qPCR was done

831 in quadruplicate for each cDNA using a LightCycler® 480 System (Roche). In parallel, a standard
832 curve was generated for each pair of qPCR primers using genomic DNA (gDNA) from *M. xanthus*
833 WT strain DK1622 and gene expression was quantified using the relative standard curve
834 method (user bulletin 2; Applied Biosystems). 16S rRNA was used as the internal standard for
835 each sample. The primers used for RT-qPCR analysis of 16S rRNA (73) and the late-acting
836 operons (26) have been described previously.
837 Relative transcript levels for mutants are the average of three biological replicates after
838 each replicate was normalized to the transcript level observed for one replicate of the WT
839 strain at the earliest time point (i.e., either 6 or 18 h PS) in the same experiment (16).
840 Transcript levels for the WT strain at other times PS were likewise normalized to that observed
841 for the WT strain at the earliest time point in the same experiment. For the WT strain at the
842 earliest time point, the transcript levels of at least three biological replicates from different
843 experiments were normalized to their average, which was set as 1.
844 To measure transcript degradation rates, samples were collected immediately after addition
845 of rifampicin (designated t_0) and 8 and 16 min later for RNA extraction and analysis as described
846 above. For each biological replicate the transcript levels after 8 and 16 min were normalized to
847 the transcript level at t_0, which was set as 1, and the natural log of the resulting values was
848 plotted versus minutes after rifampicin treatment (16). The slope of a linear fit of the data was
849 used to compute the mRNA half-life.
850
851 ***Expression and purification of proteins***

852 To express His-tagged proteins, *E. coli* strain BL21(DE3) was transformed with pET11a/FruA-
853 DBD-H_8, pET11km/FruA-H_6, or pPH158 (for H_6-MrpC) and transformants were selected on LB
854 1.5% agar containing 50 μg/mL ampicillin or kanamycin sulfate. In each case, a single colony
855 was used to inoculate 10 mL of LB supplemented with antibiotic, followed by overnight
856 incubation at 37°C with shaking. Five mL of overnight culture was used to inoculate 500 mL of
857 the same medium, followed by continued shaking at 37°C until the culture reached 60-80 Klett
858 units. IPTG (1 mM final concentration) was added to induce synthesis of the recombinant
859 protein. After 2 h, cells were harvested as reported previously (57) and stored at -80°C.
860 To purify His-tagged proteins, a modification of a protocol described previously (74) was
861 used. Each cell pellet was resuspended in 35 mL of lysis buffer (50 mM Na-phosphate buffer pH
862 8.0, 500 mM NaCl, 14 mM β-mercaptoethanol, protease inhibitors [1 Roche Mini EDTA-free
863 tablet/10 mL]). Cells were disrupted by sonication (4 times for 1 min with intermittent cooling
864 on ice). After centrifugation at 18,000 × *g* for 10 min at 4°C, the supernatant was mixed with 5
865 mL of lysis buffer containing 10% w/v Triton X-100, 1 mL of 1 M imidazole (pH 8.0), enough lysis
866 buffer for 50 mL total, and finally 0.5 mL of Ni-NTA agarose (Qiagen) that had been washed 3
867 times with lysis buffer containing 20 mM imidazole. The mixture was rotated for 1 h at 4°C.
868 The Ni-NTA agarose was collected by centrifugation at 700 × *g* for 3 min at 4°C and washed 4
869 times with 50 mL of lysis buffer containing 20 mM imidazole, 0.5% w/v Triton X-100, and 25%
870 w/v glycerol. The Ni-NTA agarose was rotated for 30 min at 4°C with 10 mL of elution buffer
871 (50 mM Na-phosphate buffer pH 8.0, 500 mM NaCl, 1.4 mM β-mercaptoethanol, protease
872 inhibitors [1 Roche Mini EDTA-free tablet], 250 mM imidazole, 0.5% w/v Triton X-100, 25% w/v
873 glycerol). Eluates were dialyzed twice at 4°C against 1 L of storage buffer (10 mM Tris-HCL pH

874 8.0, 100 mM NaCl, 1 mM β-mercaptoethanol, 10% w/v glycerol) and aliquots were stored at -
875 80°C. The protein concentration was determined using a Bradford (75) assay kit (Bio-Rad).
876 To express MBP-Nla6 DBD, *E. coli* strain BL21(DE3) was transformed with pMAL-c5x/MBP-
877 Nla6 DBD and transformants were selected on LB 1.5% agar containing 100 μg/mL ampicillin.
878 Five colonies were used to inoculate 80 mL of LB supplemented with antibiotic and 0.2%
879 dextrose, followed by incubation at 37°C with shaking at 350 rpm until the culture reached 60
880 Klett units. IPTG (0.3 mM final concentration) was added to induce synthesis of the
881 recombinant protein. After 2 h, cells were harvested, the cell pellet was resuspended in 10 mL
882 of column buffer (20 mM Tris-HCl pH 7.5, 200 mM NaCl, 1 mM EDTA, protease inhibitors [1
883 Roche Mini EDTA-free tablet], 10 mM β-mercaptoethanol), and the cell suspension was stored
884 at -20°C.
885 MBP-Nla6 DBD was purified according to instructions in the pMAL™ Protein Fusion &
886 Purification System manual (NEB). Briefly, the cell pellet was thawed and cells were disrupted
887 by sonication (8 times for 15 s with intermittent cooling on ice). After centrifugation at 18,000
888 × *g* for 20 min at 4°C, the supernatant was loaded onto a 1 mL amylose gravity-flow column,
889 which had been prewashed with 5 mL of column buffer. The loaded column was washed with
890 12 mL of column buffer, then eluted with 2.5 mL of column buffer supplemented with 10 mM
891 maltose, collecting fractions of 4 drops each (approximately 200 μL). Fractions were subjected
892 to SDS-PAGE with Coomassie Blue staining. Fractions 4-9, with maximal purified MBP-Nla6
893 DBD, were pooled, dialyzed as described above, and aliquots were stored at -80°C. The protein
894 concentration was determined by measuring the absorbance at 280 nm and using the
895 calculated extinction coefficient of MBP-Nla6 DBD (1.32 $[mg/mL]^{-1}cm^{-1}$).

896

897 ***Electrophoretic mobility shift assays***

898 ^{32}P-labelled DNA fragments were generated by PCR using primers labelled with [γ-^{32}P]ATP using
899 T4 polynucleotide kinase (NEB) according to the manufacturer's instructions. The templates for
900 PCR were either plasmid DNA or gDNA from *M. xanthus* WT strain DK1622. The primers and
901 templates were as follows: primers LK1298 and LK1331 with template pPV391 for *dev*, primers
902 *exoA-I* -171 fwd and *exoA-I* -1 rev with template gDNA for *exoA-I*, primers *fadIJ* -214 fwd and
903 *fadIJ* -5 rev with template gDNA for *fadIJ*, primers *exoL-P* -217 fwd and *exoL-P* +56 rev with
904 template gDNA for *exoL-P*, and primers *nfsA-H* -166 fwd and *nfsA-H* +35 with template pSS14
905 for *nfsA-H.* The labeled DNA fragments were purified by electrophoresis on 15%
906 polyacrylamide gels, followed by visualization using autoradiography, excision, and overnight
907 elution by soaking in TE buffer (10 mM Tris-HCl pH 8.0, 1 mM EDTA) as described previously
908 (57).

909 Binding reactions (10 μL) were performed as reported previously (57), except the reaction
910 mixtures were incubated at 37°C for 10 min prior to loading on 8% polyacrylamide gels. To
911 determine whether the order of protein addition was important, one protein was added to the
912 reaction mixture during an initial 10 min incubation at 37°C, followed by addition of a second
913 protein and another 10 min incubation at 37°C, prior to loading on 8% polyacrylamide gels.
914 Gels were dried and exposed to X-ray film for autoradiography as described (57).

915

916 **Acknowledgments**

917 We thank Monique Floer for advice about high-throughput qPCR and for use of the LightCycler®
918 480 System. We thank Anthony Garza, Lawrence Shimkets, Ramya Rajagopalan, Wenyuan Shi,
919 Sumiko Inouye, Montserrat Elias-Arnanz, and Penelope Higgs for sharing strains. We thank
920 Muqing Ma and Anthony Garza for constructing pMAL-c5x/MBP-ΔCNla6 DBD. This work was
921 supported by the National Science Foundation (awards MCB-1411272 and IOS-1951025) and by
922 salary support for L.K. from Michigan State University AgBioResearch.

923

924 **Author contributions**

925 Conception or design of the study: LK, SS

926 Acquisition of the data: SS, LK

927 Analysis or interpretation of the data: SS, LK

928 Writing of the manuscript: LK, SS

929

930 **References**

931 1. Yang Z, Higgs P, editors. Myxobacteria: genomics, cellular and molecular biology. Norfolk, UK:
932 Caister Academic Press; 2014.
933 2. O'Connor KA, Zusman DR. Behavior of peripheral rods and their role in the life cycle of *Myxococcus*
934 *xanthus*. J Bacteriol. 1991;173(11):3342-55.
935 3. Lee B, Holkenbrink C, Treuner-Lange A, Higgs PI. *Myxococcus xanthus* developmental cell fate
936 production: heterogeneous accumulation of developmental regulatory proteins and reexamination
937 of the role of MazF in developmental lysis. J Bacteriol. 2012;194(12):3058-68.
938 4. Kroos L. Highly signal-responsive gene regulatory network governing *Myxococcus* development.
939 Trends Genet. 2017;33:3-15.
940 5. Harris BZ, Kaiser D, Singer M. The guanosine nucleotide (p)ppGpp initiates development and A-
941 factor production in *Myxococcus xanthus*. Genes Dev. 1998;12(7):1022-35.
942 6. Manoil C, Kaiser D. Accumulation of guanosine tetraphosphate and guanosine pentaphosphate in
943 *Myxococcus xanthus* during starvation and myxospore formation. J Bacteriol. 1980;141:297-304.
944 7. Skotnicka D, Smaldone GT, Petters T, Trampari E, Liang J, Kaever V, et al. A minimal threshold of c-di-
945 GMP is essential for fruiting body formation and sporulation in *Myxococcus xanthus*. PLoS Genet.
946 2016;12(5):e1006080.

947 8. Crawford EW, Jr., Shimkets LJ. The *Myxococcus xanthus socE* and *csgA* genes are regulated by the
948 stringent response. Mol Microbiol. 2000;37(4):788-99.
949 9. Konovalova A, Lobach S, Sogaard-Andersen L. A RelA-dependent two-tiered regulated proteolysis
950 cascade controls synthesis of a contact-dependent intercellular signal in *Myxococcus xanthus*. Mol
951 Microbiol. 2012;84(2):260-75.
952 10. Konovalova A, Wegener-Feldbrugge S, Sogaard-Andersen L. Two intercellular signals required for
953 fruiting body formation in *Myxococcus xanthus* act sequentially but non-hierarchically. Mol
954 Microbiol. 2012;86(1):65-81.
955 11. Kim SK, Kaiser D. C-factor: a cell-cell signaling protein required for fruiting body morphogenesis of
956 *M. xanthus*. Cell. 1990;61:19-26.
957 12. Lobedanz S, Sogaard-Andersen L. Identification of the C-signal, a contact-dependent morphogen
958 coordinating multiple developmental responses in *Myxococcus xanthus*. Genes Dev.
959 2003;17(17):2151-61.
960 13. Rolbetzki A, Ammon M, Jakovljevic V, Konovalova A, Sogaard-Andersen L. Regulated secretion of a
961 protease activates intercellular signaling during fruiting body formation in *M. xanthus*. Dev Cell.
962 2008;15(4):627-34.
963 14. Boynton TO, Shimkets LJ. *Myxococcus* CsgA, *Drosophila* Sniffer and human HSD17B10 are cardiolipin
964 phospholipases. Genes Dev. 2015;29:1903-14.
965 15. Ellehauge E, Norregaard-Madsen M, Sogaard-Andersen L. The FruA signal transduction protein
966 provides a checkpoint for the temporal co-ordination of intercellular signals in *Myxococcus xanthus*
967 development. Mol Microbiol. 1998;30:807-17.
968 16. Saha S, Patra P, Igoshin O, Kroos L. Systematic analysis of the *Myxococcus xanthus* developmental
969 gene regulatory network supports posttranslational regulation of FruA by C-signaling. Mol Microbiol.
970 2019;111:1732-52.
971 17. Ogawa M, Fujitani S, Mao X, Inouye S, Komano T. FruA, a putative transcription factor essential for
972 the development of *Myxococcus xanthus*. Mol Microbiol. 1996;22(4):757-67.
973 18. Mittal S, Kroos L. A combination of unusual transcription factors binds cooperatively to control
974 *Myxococcus xanthus* developmental gene expression. Proc Natl Acad Sci USA. 2009;106:1965-70.
975 19. Giglio KM, Caberoy N, Suen G, Kaiser D, Garza AG. A cascade of coregulating enhancer binding
976 proteins initiates and propagates a multicellular developmental program. Proc Natl Acad Sci USA.
977 2011;108:E431-E9.
978 20. Ueki T, Inouye S. Identification of an activator protein required for the induction of *fruA*, a gene
979 essential for fruiting body development in *Myxococcus xanthus*. Proc Natl Acad Sci USA.
980 2003;100(15):8782-7.
981 21. Nariya H, Inouye S. A protein Ser/Thr kinase cascade negatively regulates the DNA-binding activity of
982 MrpC, a smaller form of which may be necessary for the *Myxococcus xanthus* development. Mol
983 Microbiol. 2006;60(5):1205-17.
984 22. McLaughlin PT, Bhardwaj V, Feeley BE, Higgs PI. MrpC, a CRP/Fnr homolog, functions as a negative
985 autoregulator during the *Myxococcus xanthus* multicellular developmental program. Mol Microbiol.
986 2018;109:245-61.
987 23. Higgs PI, Jagadeesan S, Mann P, Zusman DR. EspA, an orphan hybrid histidine protein kinase,
988 regulates the timing of expression of key developmental proteins of *Myxococcus xanthus*. J
989 Bacteriol. 2008;190:4416-26.
990 24. Schramm A, Lee B, Higgs PI. Intra- and inter-protein phosphorylation between two hybrid histidine
991 kinases controls *Myxococcus xanthus* developmental progression. J Biol Chem. 2012;287:25060–72.
992 25. Rajagopalan R, Kroos L. Nutrient-regulated proteolysis of MrpC halts expression of genes important
993 for commitment to sporulation during *Myxococcus xanthus* development. J Bacteriol.
994 2014;196:2736-47.

995 26. Hoang Y, Kroos L. Ultrasensitive response of developing *Myxococcus xanthus* to the addition of
996 nutrient medium correlates with the level of MrpC. J Bacteriol. 2018;200:e00456-18.
997 27. Robinson M, Son B, Kroos L. Transcription factor MrpC binds to promoter regions of many
998 developmentally-regulated genes in *Myxococcus xanthus*. BMC Genomics. 2014;15:1123.
999 28. Campbell A, Viswanathan P, Barrett T, Son B, Saha S, Kroos L. Combinatorial regulation of the *dev*
1000 operon by MrpC2 and FruA during *Myxococcus xanthus* development. J Bacteriol. 2015;197:240-51.
1001 29. Lee J, Son B, Viswanathan P, Luethy P, Kroos L. Combinatorial regulation of *fmgD* by MrpC2 and FruA
1002 during *Myxococcus xanthus* development. J Bacteriol. 2011;193:1681-9.
1003 30. Mittal S, Kroos L. Combinatorial regulation by a novel arrangement of FruA and MrpC2 transcription
1004 factors during *Myxococcus xanthus* development. J Bacteriol. 2009;191:2753-63.
1005 31. Son B, Liu Y, Kroos L. Combinatorial regulation by MrpC2 and FruA involves three sites in the *fmgE*
1006 promoter region during *Myxococcus xanthus* development. J Bacteriol. 2011;193:2756-66.
1007 32. Kroos L, Kaiser D. Expression of many developmentally regulated genes in *Myxococcus* depends on a
1008 sequence of cell interactions. Genes Dev. 1987;1:840-54.
1009 33. Hoang Y, Franklin JL, Dufour YS, Kroos L. Cell density, alignment, and orientation correlate with C-
1010 signal-dependent gene expression during *Myxococcus xanthus* development. Proc Natl Acad Sci USA.
1011 2021;118(45):e2111706118.
1012 34. Kim SK, Kaiser D. Cell alignment required in differentiation of *Myxococcus xanthus*. Science.
1013 1990;249:926-8.
1014 35. Kroos L, Kuspa A, Kaiser D. A global analysis of developmentally regulated genes in *Myxococcus*
1015 *xanthus*. Dev Biol. 1986;117:252-66.
1016 36. Kroos L, Kuspa A, Kaiser D. Defects in fruiting body development caused by Tn*5 lac* insertions in
1017 *Myxococcus xanthus*. J Bacteriol. 1990;172:484-7.
1018 37. Boysen A, Ellehauge E, Julien B, Sogaard-Andersen L. The DevT protein stimulates synthesis of FruA,
1019 a signal transduction protein required for fruiting body morphogenesis in *Myxococcus xanthus*. J
1020 Bacteriol. 2002;184(6):1540-6.
1021 38. Thony-Meyer L, Kaiser D. *devRS*, an autoregulated and essential genetic locus for fruiting body
1022 development in *Myxococcus xanthus*. J Bacteriol. 1993;175:7450-62.
1023 39. Viswanathan P, Murphy K, Julien B, Garza AG, Kroos L. Regulation of *dev*, an operon that includes
1024 genes essential for *Myxococcus xanthus* development and CRISPR-associated genes and repeats. J
1025 Bacteriol. 2007;189:3738-50.
1026 40. Rajagopalan R, Wielgoss S, Lippert G, Velicer GJ, Kroos L. *devI* is an evolutionarily young negative
1027 regulator of *Myxococcus xanthus* development. J Bacteriol. 2015;197(7):1249-62.
1028 41. Rajagopalan R, Kroos L. The *dev* operon regulates the timing of sporulation during *Myxococcus*
1029 *xanthus* development. J Bacteriol. 2017;199(10):e00788-16.
1030 42. Bullock HA, Shen H, Boynton TO, Shimkets LJ. Fatty acid oxidation is required for *Myxococcus*
1031 *xanthus* development. J Bacteriol. 2018;200(10):e00572-17.
1032 43. Kuzmich S, Blumenkamp P, Meier D, Szadkowski D, Goesmann A, Becker A, et al. CRP-Like
1033 transcriptional regulator MrpC curbs c-di-GMP and 3',3'-cGAMP nucleotide levels during
1034 development in *Myxococcus xanthus*. mBio. 2022;13:e00044-22.
1035 44. Muller FD, Treuner-Lange A, Heider J, Huntley SM, Higgs PI. Global transcriptome analysis of spore
1036 formation in *Myxococcus xanthus* reveals a locus necessary for cell differentiation. BMC Genomics.
1037 2010;11:264.
1038 45. Muller FD, Schink CW, Hoiczyk E, Cserti E, Higgs PI. Spore formation in *Myxococcus xanthus* is tied to
1039 cytoskeleton functions and polysaccharide spore coat deposition. Mol Microbiol. 2012;83(3):486-
1040 505.
1041 46. Holkenbrink C, Hoiczyk E, Kahnt J, Higgs PI. Synthesis and assembly of a novel glycan layer in
1042 *Myxococcus xanthus* spores. J Biol Chem. 2014;289(46):32364-78.

1043 47. Wartel M, Ducret A, Thutupalli S, Czerwinski F, Le Gall AV, Mauriello EM, et al. A versatile class of
1044 cell surface directional motors gives rise to gliding motility and sporulation in *Myxococcus xanthus*.
1045 PLoS Biol. 2013;11(12):e1001728.
1046 48. Licking E, Gorski L, Kaiser D. A common step for changing cell shape in fruiting body and starvation-
1047 independent sporulation of *Myxococcus xanthus*. J Bacteriol. 2000;182(12):3553-8.
1048 49. Ueki T, Inouye S. Identification of a gene involved in polysaccharide export as a transcription target
1049 of FruA, an essential factor for *Myxococcus xanthus* development. J Biol Chem. 2005;280(37):32279-
1050 84.
1051 50. Giglio KM, Zhu C, Klunder C, Kummer S, Garza AG. The enhancer binding protein Nla6 regulates
1052 developmental genes that are important for *Myxococcus xanthus* sporulation. J Bacteriol.
1053 2015;197(7):1276-87.
1054 51. Perez-Burgos M, Garcia-Romero I, Valvano MA, Sogaard Andersen L. Identification of the Wzx
1055 flippase, Wzy polymerase and sugar-modifying enzymes for spore coat polysaccharide biosynthesis
1056 in *Myxococcus xanthus*. Mol Microbiol. 2020;113(6):1189-208.
1057 52. Kaiser D. Social gliding is correlated with the presence of pili in *Myxococcus xanthus*. Proc Natl Acad
1058 Sci USA. 1979;76:5952-6.
1059 53. Caberoy NB, Welch RD, Jakobsen JS, Slater SC, Garza AG. Global mutational analysis of NtrC-like
1060 activators in *Myxococcus xanthus*: identifying activator mutants defective for motility and fruiting
1061 body development. J Bacteriol. 2003;185(20):6083-94.
1062 54. Cuthbertson L, Mainprize IL, Naismith JH, Whitfield C. Pivotal roles of the outer membrane
1063 polysaccharide export and polysaccharide copolymerase protein families in export of extracellular
1064 polysaccharides in gram-negative bacteria. Microbiol Mol Biol Rev. 2009;73(1):155-77.
1065 55. McLoon AL, Boeck ME, Bruckskotten M, Keyel AC, Sogaard-Andersen L. Transcriptomic analysis of
1066 the *Myxococcus xanthus* FruA regulon, and comparative developmental transcriptomic analysis of
1067 two fruiting body forming species, *Myxococcus xanthus* and *Myxococcus stipitatus*. BMC Genomics.
1068 2021;22(1):784.
1069 56. Viswanathan P, Ueki T, Inouye S, Kroos L. Combinatorial regulation of genes essential for
1070 *Myxococcus xanthus* development involves a response regulator and a LysR-type regulator. Proc
1071 Natl Acad Sci USA. 2007;104:7969-74.
1072 57. Yoder-Himes D, Kroos L. Regulation of the *Myxococcus xanthus* C-signal-dependent Ω4400
1073 promoter by the essential developmental protein FruA. J Bacteriol. 2006;188:5167-76.
1074 58. Viswanathan K, Viswanathan P, Kroos L. Mutational analysis of the *Myxococcus xanthus* Ω4406
1075 promoter region reveals an upstream negative regulatory element that mediates C-signal
1076 dependence. J Bacteriol. 2006;188:515-24.
1077 59. Munoz-Dorado J, Inouye S, Inouye M. A gene encoding a protein serine/threonine kinase is required
1078 for normal development of *M. xanthus*, a Gram-negative bacterium. Cell. 1991;67:995-1006.
1079 60. Kroos L. Eukaryotic-like signaling and gene regulation in a prokaryote that undergoes multicellular
1080 development. Proc Natl Acad Sci USA. 2005;102(8):2681-2.
1081 61. Davidson EH. Genomic Regulatory Systems. San Diego: Academic Press; 2001.
1082 62. Volz C, Kegler C, Muller R. Enhancer binding proteins act as hetero-oligomers and link secondary
1083 metabolite production to myxococcal development, motility, and predation. Chem Biol.
1084 2012;19(11):1447-59.
1085 63. Eichenberger P, Fujita M, Jensen ST, Conlon EM, Rudner DZ, Wang ST, et al. The program of gene
1086 transcription for a single differentiating cell type during sporulation in *Bacillus subtilis*. PLoS Biol.
1087 2004;2(10):1664-83.
1088 64. Kroos L. The *Bacillus* and *Myxococcus* developmental networks and their transcriptional regulators.
1089 Ann Rev Genet. 2007;41:13-39.

1090 65. Arrieta-Ortiz ML, Hafemeister C, Bate AR, Chu T, Greenfield A, Shuster B, et al. An experimentally
1091 supported model of the *Bacillus subtilis* global transcriptional regulatory network. Mol Syst Biol.
1092 2015;11(11):839.
1093 66. McKenney PT, Driks A, Eichenberger P. The *Bacillus subtilis* endospore: assembly and functions of
1094 the multilayered coat. Nat Rev Microbiol. 2013;11(1):33-44.
1095 67. Shuster B, Khemmani M, Abe K, Huang X, Nakaya Y, Maryn N, et al. Contributions of crust proteins
1096 to spore surface properties in *Bacillus subtilis*. Mol Microbiol. 2019;111(3):825-43.
1097 68. Shuster B, Khemmani M, Nakaya Y, Holland G, Iwamoto K, Abe K, et al. Expansion of the spore
1098 surface polysaccharide layer in *Bacillus subtilis* by deletion of genes encoding glycosyltransferases
1099 and glucose modification enzymes. J Bacteriol. 2019;201(19):e00321-19.
1100 69. Kashefi K, Hartzell P. Genetic supression and phenotypic masking of a *Myxococcus xanthux frzF*$^-$
1101 defect. Molec Microbiol. 1995;15:483-94.
1102 70. Iniesta AA, Garcia-Heras F, Abellon-Ruiz J, Gallego-Garcia A, Elias-Arnanz M. Two systems for
1103 conditional gene expression in *Myxococcus xanthus* inducible by isopropyl-β-D-
1104 thiogalactopyranoside or vanillate. J Bacteriol. 2012;194(21):5875-85.
1105 71. Gibson DG, Young L, Chuang RY, Venter JC, Hutchison CA, 3rd, Smith HO. Enzymatic assembly of DNA
1106 molecules up to several hundred kilobases. Nat Methods. 2009;6(5):343-5.
1107 72. Sambrook J, Fritsch E, Maniatis T. Molecular Cloning: a laboratory manual, 2nd ed. Cold Spring
1108 Harbor: Cold Spring Harbor Laboratory Press; 1989.
1109 73. Ossa F, Diodati ME, Caberoy NB, Giglio KM, Edmonds M, Singer M, et al. The *Myxococcus xanthus*
1110 Nla4 protein is important for expression of stringent response-associated genes, ppGpp
1111 accumulation, and fruiting body development. J Bacteriol. 2007;189(23):8474-83.
1112 74. Nariya H, Inouye S. Identification of a protein Ser/Thr kinase cascade that regulates essential
1113 transcriptional activators in *Myxococcus xanthus* development. Mol Microbiol. 2005;58(2):367-79.
1114 75. Bradford M. A rapid and sensitive method for the quantitation of microgram quantities of protein
1115 utilizing the principle of protein-dye binding. Anal Biochem. 1976;72:248-54.
1116 76. Rajagopalan R, Sarwar Z, Garza AG, Kroos L. Developmental gene regulation. In: Yang Z, Higgs P,
1117 editors. Myxobacteria: genomics, cellular and molecular biology. Norfolk, UK: Caister Academic
1118 Press; 2014. p. 105-26.
1119 77. Sun H, Shi W. Analyses of *mrp* genes during *Myxococcus xanthus* development. J Bacteriol.
1120 2001;183(23):6733-9.
1121 78. Kim SK, Kaiser D. Cell motility is required for the transmission of C-factor, an intercellular signal that
1122 coordinates fruiting body morphogenesis of *Myxococcus xanthus*. Genes Dev. 1990;4:896-905.
1123 79. Kroos L, Hartzell P, Stephens K, Kaiser D. A link between cell movement and gene expression argues
1124 that motility is required for cell-cell signaling during fruiting body development. Genes Dev.
1125 1988;2:1677-85.

1126

1127 **Supporting information captions**

1128 **Table S1 Cell and spore numbers**

1129

1130 **Table S2 Fold change in transcript levels in a *fruA* mutant relative to a WT strain for genes in**
1131 **late-acting operons based on McLoon *et al.* 2021**

1132

1133 **Table S3 Fold decrease in transcript levels in a *fruA* mutant relative to a WT strain for *dev* and**
1134 ***fmg* genes based on McLoon *et al.* 2021**

1135
1136 **Table S4 Strains, plasmids and primers**
1137
1138 **Figure S1. Sonication-sensitive cells during *M. xanthus* development.**
1139
1140 **Figure S2. Transcript levels during *M. xanthus* development.**
1141
1142 **Figure S3. Transcript stability.**
1143
1144 **Figure S4. Protein levels during *M. xanthus* development.**
1145
1146 **Figure S5. Early development of *M. xanthus* strains.**
1147
1148 **Figure S6. Late development of *M. xanthus* strains.**
1149
1150 **Figure S7. Features of promoter region DNA fragments used in DNA-binding assays.**
1151
1152 **Figure S8. Binding of the Nla6 DBD, MrpC, FruA, and the FruA DBD to the promoter regions of**
1153 **the late-acting operons.**
1154
1155 **Figure S9. DNA sequences in the promoter regions of late-acting operons match consensus**
1156 **sequences for binding of MrpC, FruA, and Nla6.**
1157

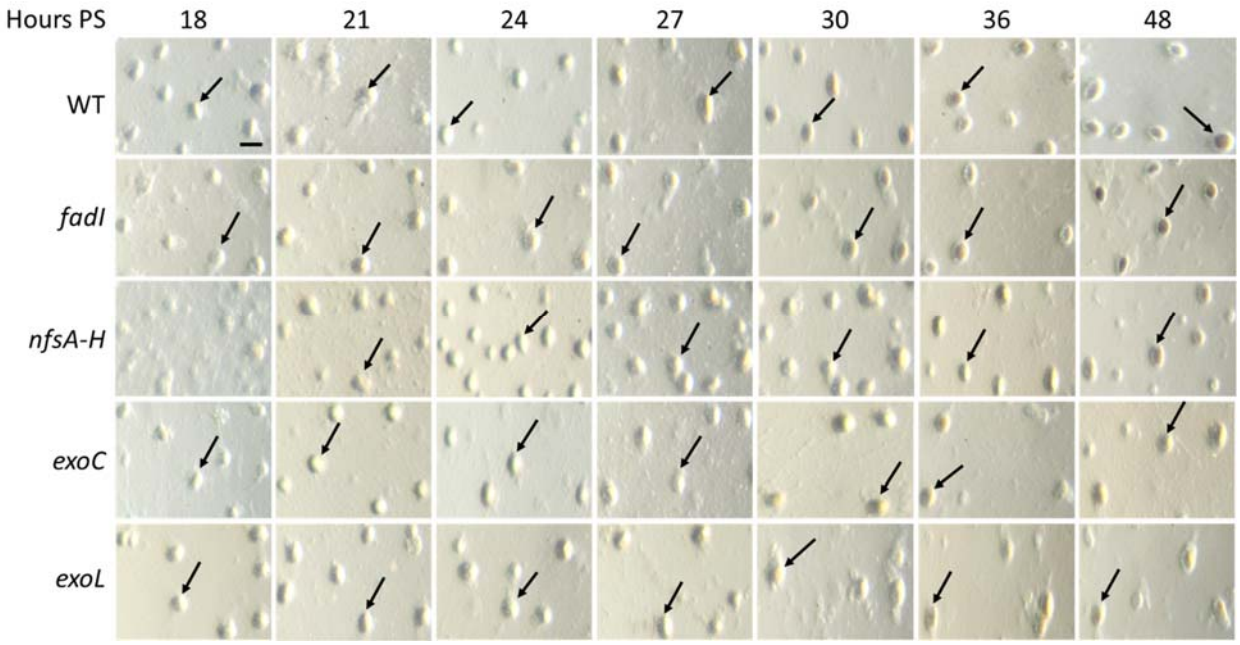

1158
1159
1160 Figure 1. Development of *M. xanthus* strains. The WT strain and its indicated mutant
1161 derivatives were subjected to starvation under submerged culture condition and microscopic
1162 images were obtained at the indicated times PS. The WT strain and all the mutants except
1163 *nfsA-H* formed compact mounds by 18 h (an arrow points to one in each panel). The *nfsA-H*
1164 mutant formed compact mounds by 21 h. Mounds of the WT strain began to darken by 30 h.
1165 Mounds of the *nfsA-H*, *exoC*, and *exoL* mutants darkened by 30 h but remained slightly less dark
1166 than mounds of the WT strain and the *fadI* mutant by 48 h. Bar, 100 μm. Similar results were
1167 observed in at least three biological replicates.
1168

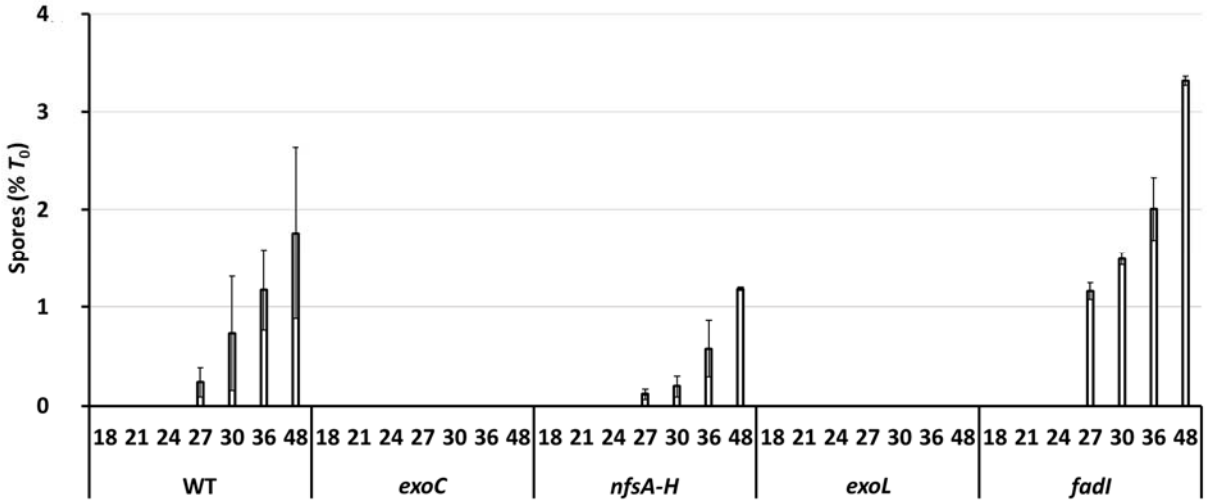

Figure 2. Sonication-resistant spores during *M. xanthus* development. The WT strain and its indicated mutant derivatives were subjected to starvation under submerged culture conditions. Samples were collected at the indicated times PS for quantification of sonication-resistant spores. Values are expressed as a percentage of the number of rod-shaped cells present at the time starvation initiated development (T_0) (Table S1). Bars show the average of three biological replicates and error bars indicate one standard deviation.

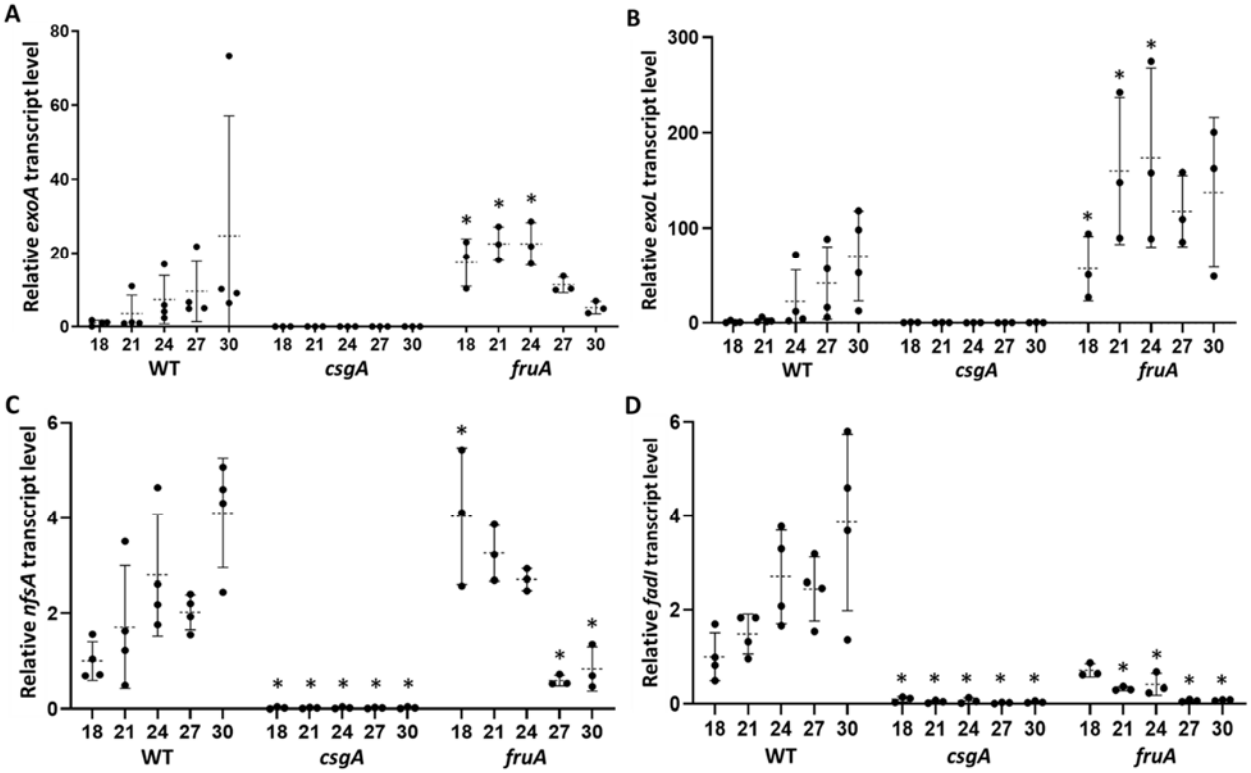

Figure 3. Transcript levels during *M. xanthus* development. The WT strain and its indicated mutant derivatives were subjected to starvation under submerged culture conditions. Samples were collected at the indicated times PS for measurement of the *exoA* (A), *exoL* (B), *nfsA* (C), and *fadI* (D) transcript levels by RT-qPCR. Graphs show the data points and the average of at least three biological replicates, relative to the WT strain at 18 h PS, and error bars indicate one standard deviation. Asterisks indicate a difference ($p < 0.05$ in Student's two-tailed *t*-tests) from the WT strain at the corresponding time PS.

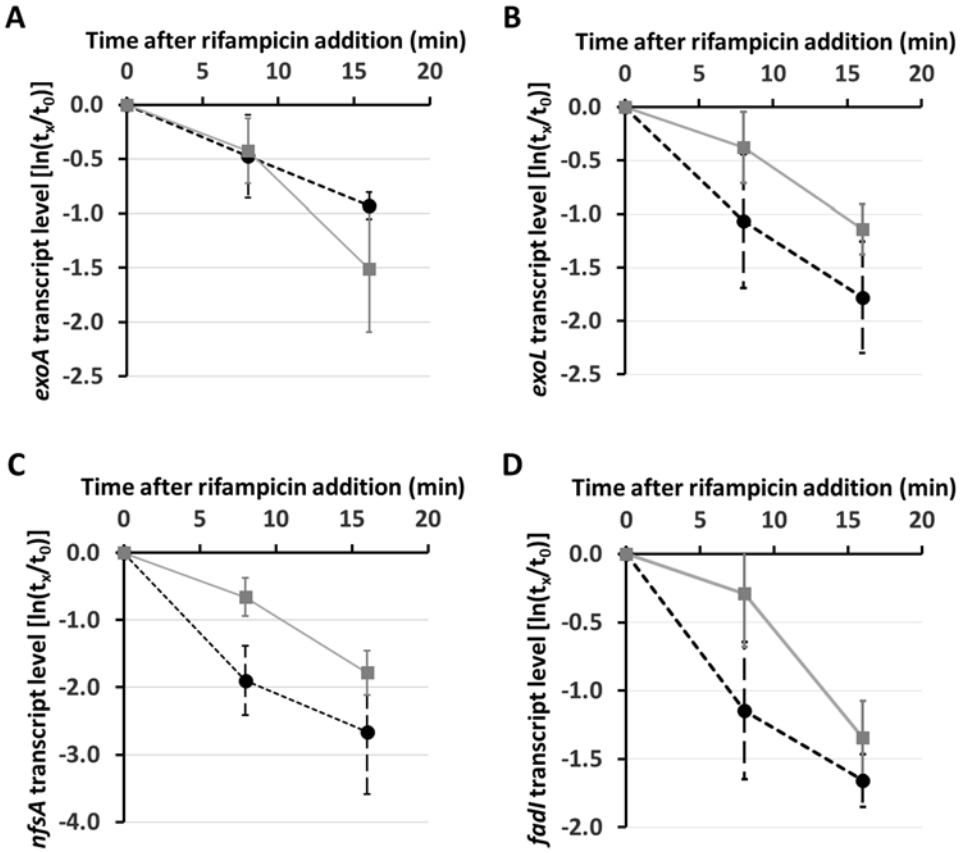

1189
1190
1191
1192

E

Transcript	Half-life in the WT strain (min)	Half-life in the *csgA* mutant (min)	*p* value
exoA	12 ± 2	8 ± 3	$p = 0.13$
exoL	8 ± 3	10 ± 2	$p = 0.20$
nfsA	5 ± 2	7 ± 1	$p = 0.26$
fadI	7 ± 1	9 ± 2	$p = 0.26$

1193
1194
1195 Figure 4. Transcript stability. The WT strain and the *csgA* mutant were subjected to starvation
1196 under submerged culture conditions for 30 h. The overlay was replaced with fresh starvation
1197 buffer containing rifampicin (50 μg/mL) and samples were collected immediately (t_0) and at the
1198 indicated times (t_x) for measurement of the *exoA* (A), *exoL* (B), *nfsA* (C), and *fadI* (D) transcript
1199 levels by RT-qPCR. Transcript levels at t_x were normalized to that at t_0 for each of three
1200 biological replicates and used to determine the transcript half-life for each replicate. The graph
1201 shows the average $\ln(t_x/t_0)$ and one standard deviation for the three biological replicates of the
1202 WT strain (black dashed line) and the *csgA* mutant (gray solid line). The average half-life and
1203 one standard deviation, as well as the *p* value from a Student's two-tailed *t*-test, are reported in
1204 (E).
1205

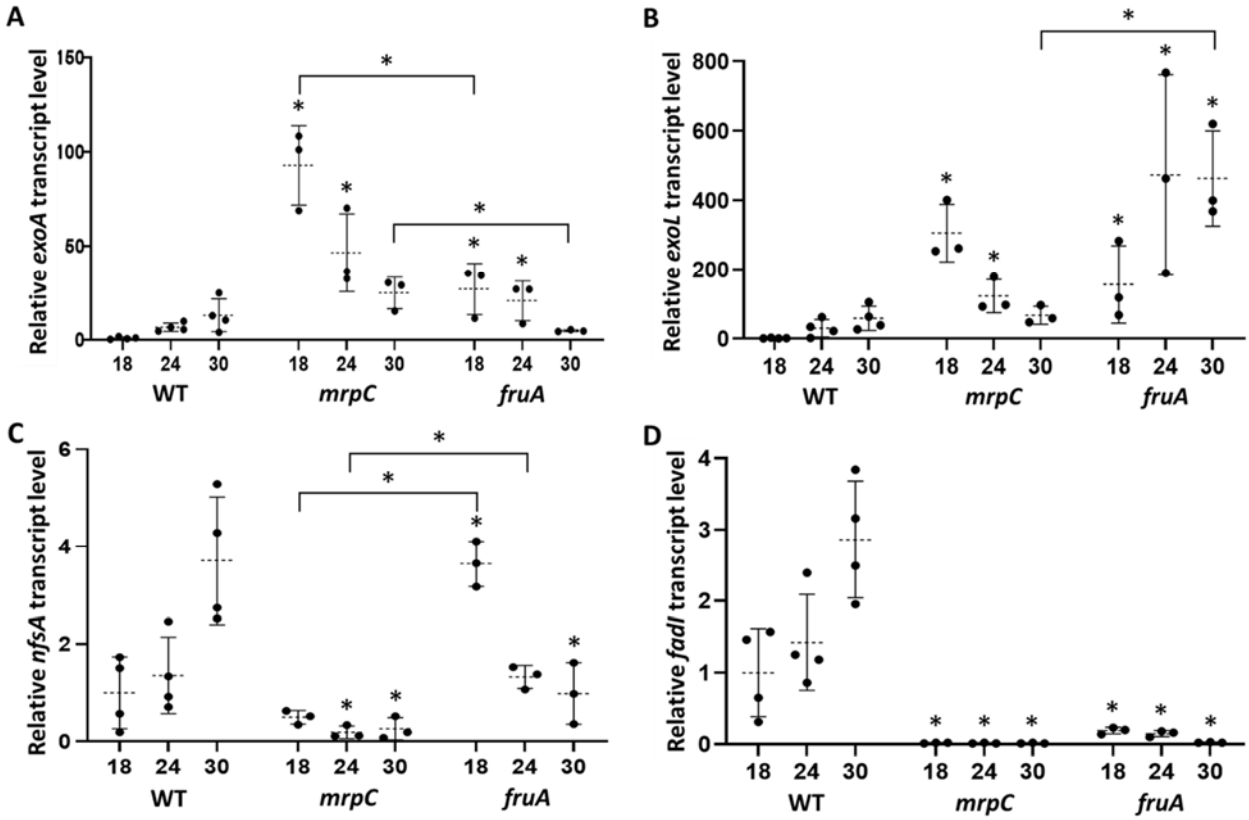

Figure 5. Transcript levels in *mrpC* and *fruA* mutants. The WT strain and its indicated mutant derivatives were subjected to starvation under submerged culture conditions. Samples were collected at the indicated times PS for measurement of *exoA* (A), *exoL* (B), *nfsA* (C), and *fadI* (D) transcript levels by RT-qPCR. Graphs show the data points and the average of at least three biological replicates, relative to the WT strain at 18 h PS, and error bars indicate one standard deviation. Asterisks above error bars indicate a difference ($p < 0.05$ in Student's two-tailed *t*-tests) from the WT strain at the corresponding time PS and asterisks above brackets indicate a difference between the mutants.

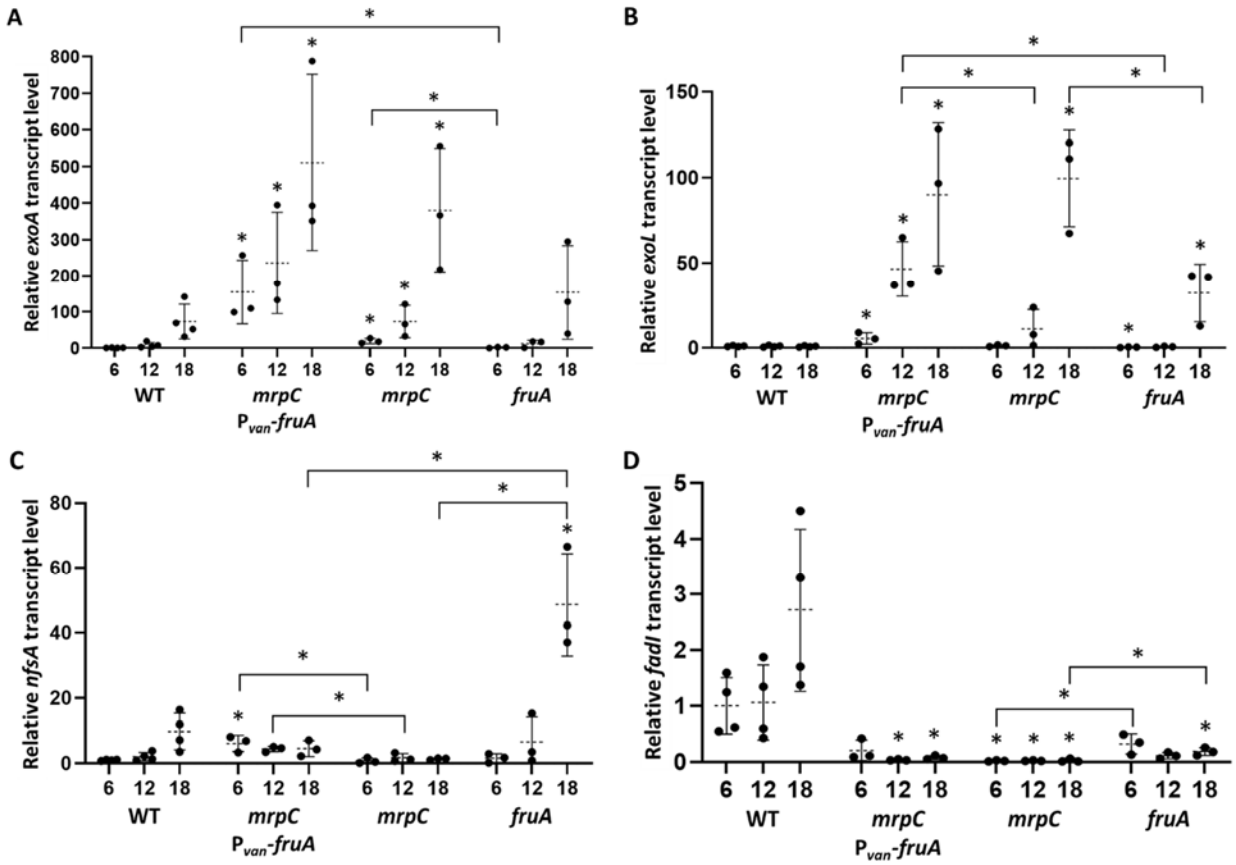

Figure 6. Transcript levels early during *M. xanthus* development. The WT strain and its indicated mutant derivatives were subjected to starvation under submerged culture conditions. Samples were collected at the indicated times PS for measurement of *exoA* (A), *exoL* (B), *nfsA* (C), and *fadI* (D) transcript levels by RT-qPCR. Graphs show the data points and the average of at least three biological replicates, relative to the WT strain at 6 h PS, and error bars indicate one standard deviation. Asterisks above error bars indicate a difference ($p < 0.05$ in Student's two-tailed *t*-tests) from the WT strain at the corresponding time PS and asterisks above brackets indicate a difference between the mutants.

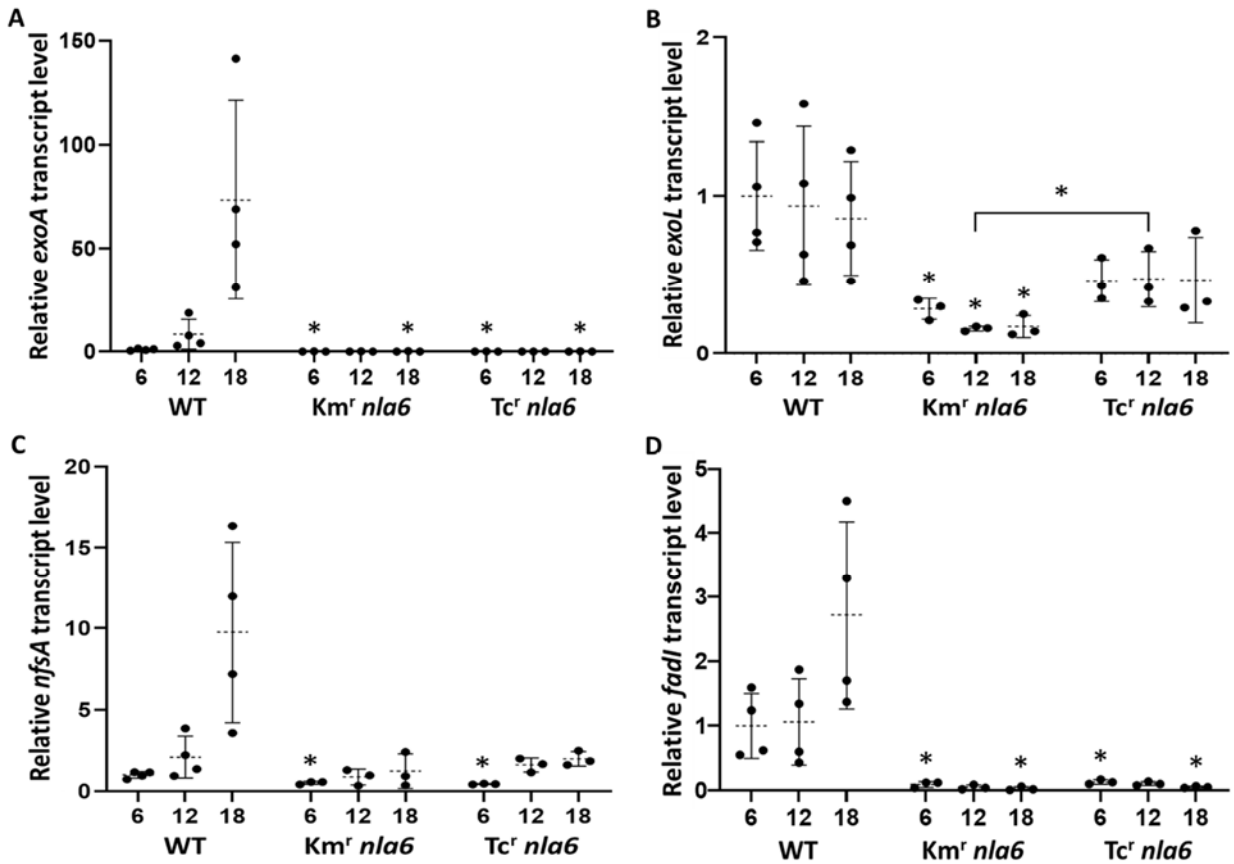

Figure 7. Transcript levels in *nla6* mutants early during *M. xanthus* development. The WT strain and its *nla6* mutant derivatives were subjected to starvation under submerged culture conditions. Samples were collected at the indicated times PS for measurement of *exoA* (A), *exoL* (B), *nfsA* (C), and *fadI* (D) transcript levels by RT-qPCR. Graphs show the data points and the average of at least three biological replicates, relative to the WT strain at 6 h PS, and error bars indicate one standard deviation. Asterisks indicate a difference ($p < 0.05$ in Student's two-tailed *t*-tests) from the WT strain at the corresponding time PS and the asterisk above the bracket indicates a difference between the mutants.

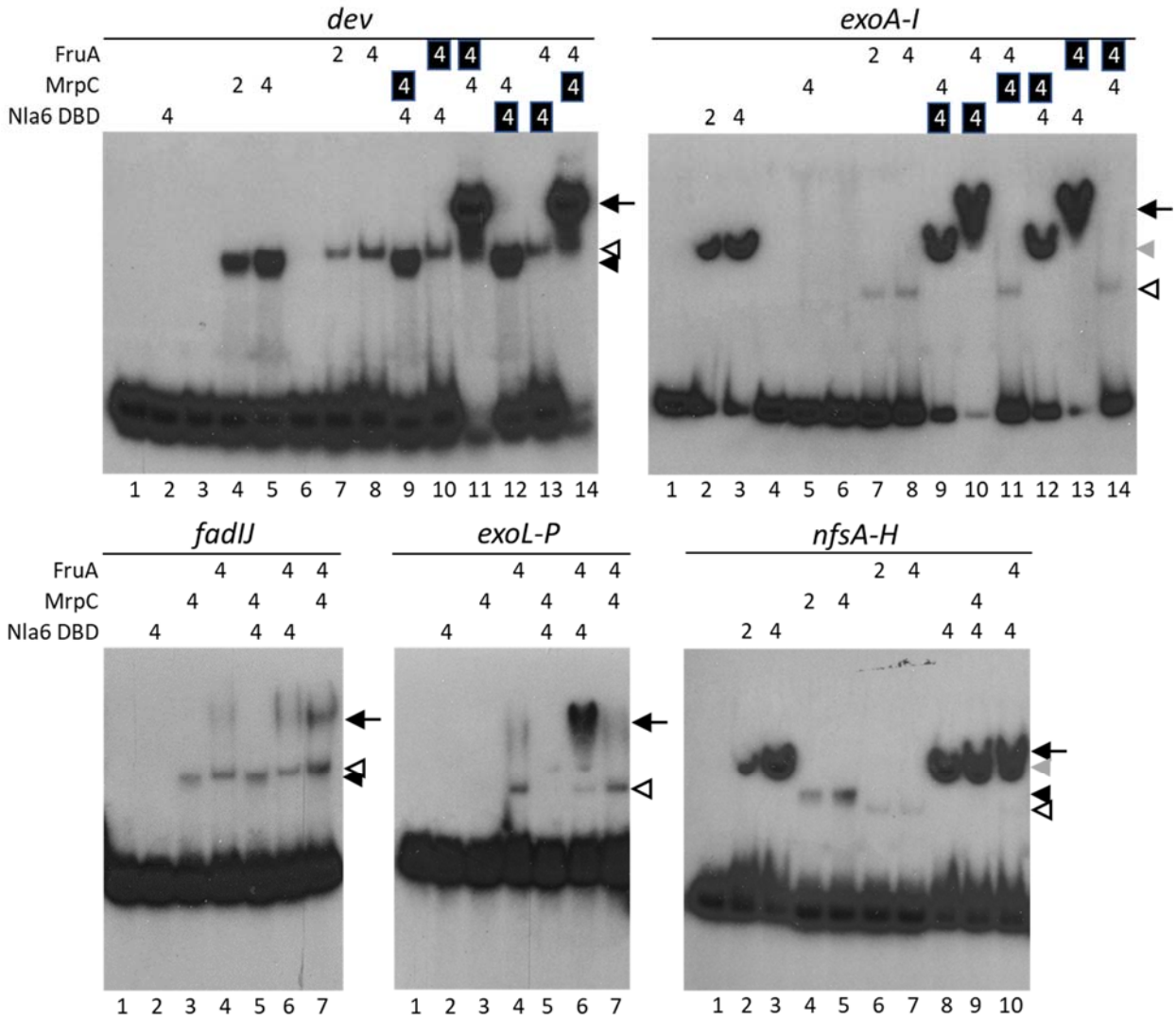

Figure 8. Binding of the Nla6 DBD, MrpC, and FruA to the promoter regions of the late-acting operons. EMSAs were performed with ^{32}P-labeled DNA fragments (2 nM) of the *dev* (-114 to -19), *exoA-I* (-171 to -1), *fadIJ* (-214 to -5), *exoL-P* (-217 to +56), and *nfsA-H* (-166 to +35) promoter regions, and MBP-Nla6 DBD, His_6-MrpC, and FruA-His_6 at the μM concentrations indicated by numbers above each autoradiographic image. A white number on a black background indicates a protein that was added to the DNA-binding reaction 10 min later than the other protein. Shifted complexes produced by MBP-Nla6 DBD alone (gray arrowheads), His_6-MrpC alone (black arrowheads), FruA-His_6 alone (white arrowheads), or binding of two proteins (arrows) are indicated. Lanes are numbered below images.

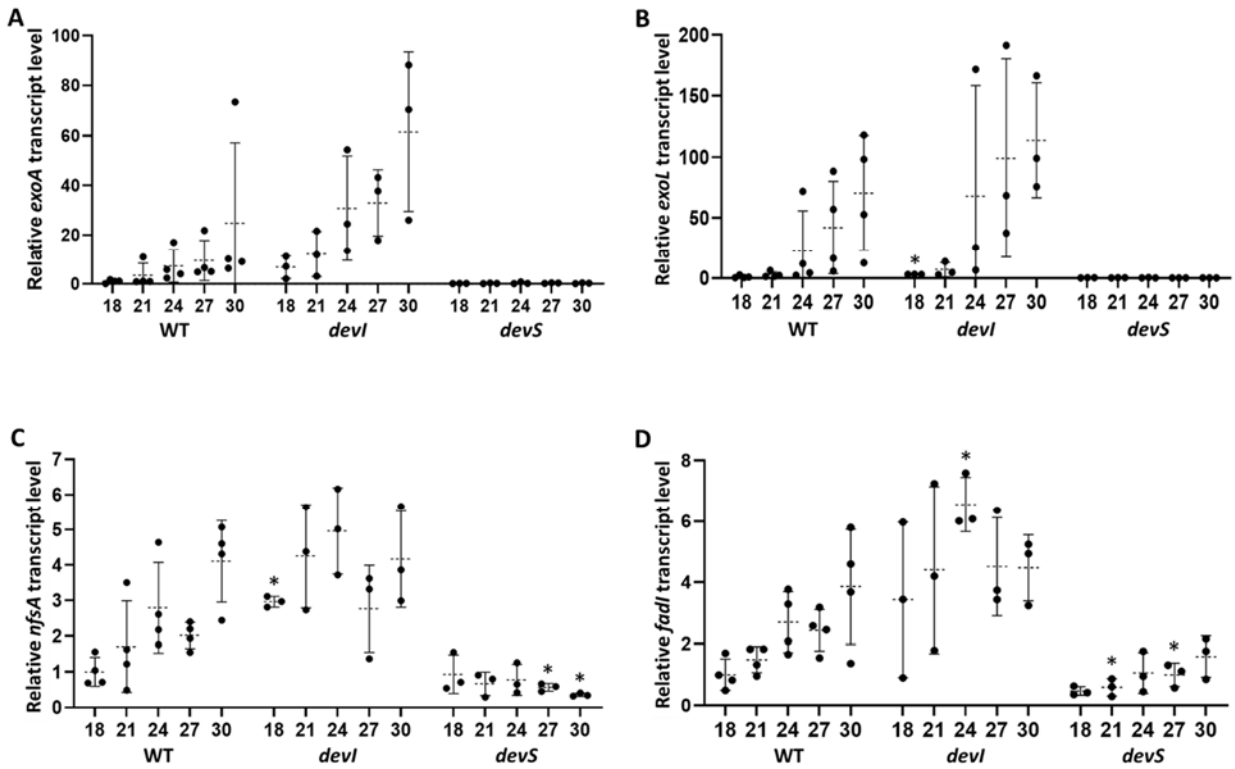

Figure 9. Transcript levels in *devI* and *devS* mutants during *M. xanthus* development. The WT strain and its *devI* and *devS* mutant derivatives were subjected to starvation under submerged culture conditions. Samples were collected at the indicated times PS for measurement of *exoA* (A), *exoL* (B), *nfsA* (C), and *fadI* (D) transcript levels by RT-qPCR. Graphs show the data points and the average of at least three biological replicates, relative to the WT strain at 18 h PS, and error bars indicate one standard deviation. Asterisks indicate a significant difference ($p < 0.05$ in Student's two-tailed *t*-tests) from the WT strain at the corresponding time PS.

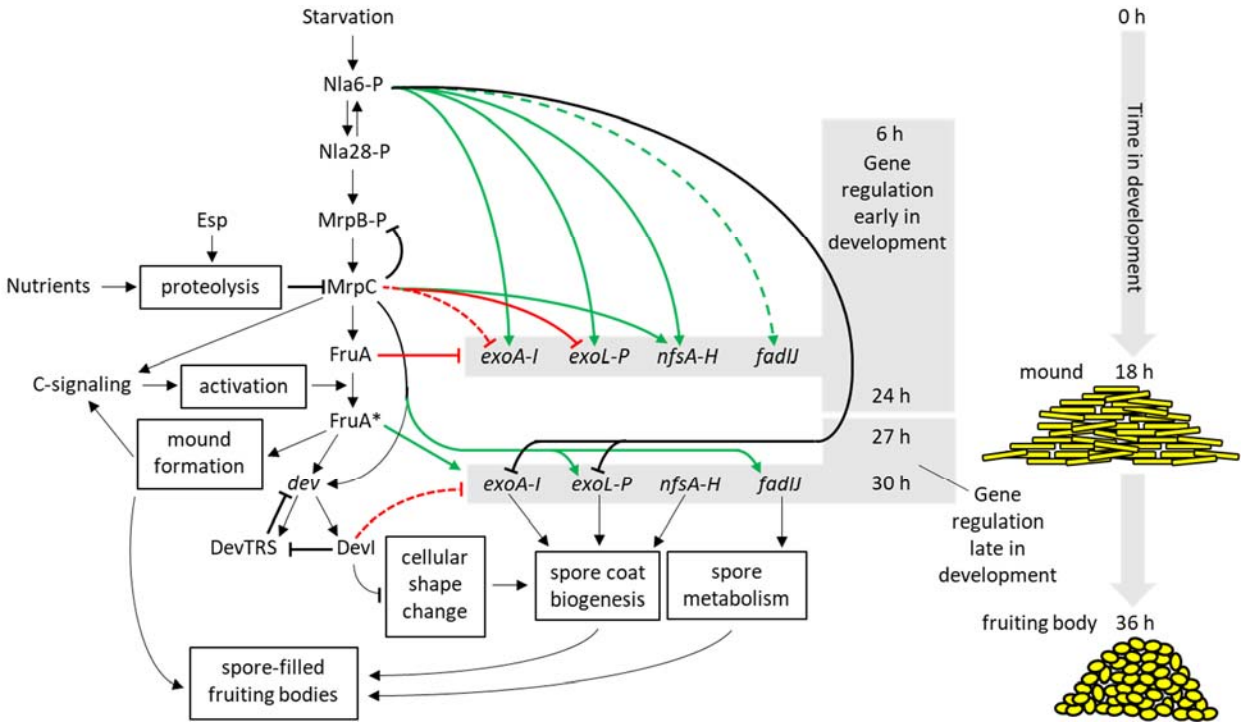

Figure 10. Model for regulation of late-acting operons during *M. xanthus* development. In response to starvation, phosphorylated Nla6 (Nla6-P) positively regulates all four late-acting operons directly (solid green arrows) or indirectly (dashed green arrow) early in development (upper gray area reflecting transcript measurements from 6-24 h PS). Nla6-P also positively regulates MrpC *via* Nla28-P (19) and MrpB-P (76). MrpC negatively regulates *exoA-I* indirectly (dashed red line with barred end) and *exoL-P* directly (solid red line with barred end), and positively regulates the *nfsA-H* operon directly, early in development. Nutrients (25, 26) and Esp signaling (23, 24) can negatively regulate MrpC *via* proteolysis, and MrpC negatively autoregulates by competing with MrpB-P for binding to the *mrpC* promoter region (22). MrpC positively regulates C-signaling (77) and *fruA* transcription (20), leading to production of unactivated FruA, which negatively regulates the late-acting operons early in development. C-signaling activates FruA to FruA* by an unknown mechanism (15, 16). FruA* positively regulates mound formation (17), which enhances C-signaling (34, 78, 79), forming a positive feedback loop. FruA* also positively regulates the *dev* operon (28, 56) and the late-acting operons late in development (lower gray area reflecting transcript measurements at 27 and 30 h). Dev TRS proteins negatively autoregulate, decreasing DevI (40, 41), which negatively regulates the late-acting operons and cellular shape change. MrpC positively regulates *dev*, *exoL-P*, and *fadIJ*, while Nla6-P negatively regulates *exoA-I* and *exoL-P* late in development. Under our submerged culture conditions, mounds form by 18 h (Fig. 1 and S5) and fruiting bodies with many spores form by 36 h (Fig. 2).